SIRMA

STRENGTHENING INFRASTRUCTURE RISK MANAGEMENT IN THE ATLANTIC AREA

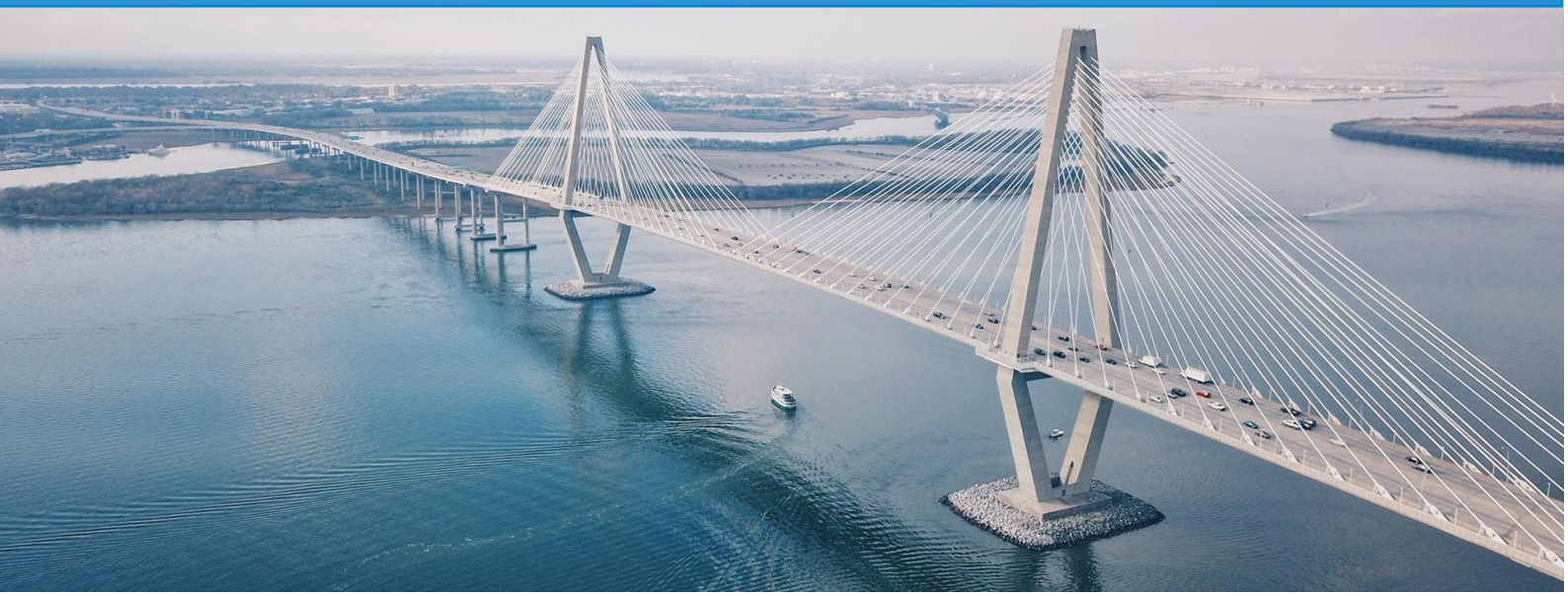

Remote Sensing in Mapping & Inspection: WP5

October 2020 (V1.0)

CONFIDENTIAL

Interreg Atlantic Area
European Regional Development Fund

EUROPEAN UNION

SIRMA@SIRMA-PROJECT.EU | WWW.SIRMA-PROJECT.EU

SIRMA

STRENGTHENING THE TERRITORY'S RESILIENCE TO RISKS OF NATURAL, CLIMATE AND HUMAN ORIGIN

Application Code: EAPA_826/2018

Remote Sensing in Mapping & Inspection

WP 5 Instrumenting Transportation Infrastructure for Extreme Natural Events

Deliverable ID	**D5.1**
Deliverable name	**Remote Sensing in Mapping & Inspection**
Lead partner	**University of Vigo (UVigo)**
Contributors	

[PUBLIC/CONFIDENTIAL]

SIRMA Project Synopsis

SIRMA aims to develop, validate and implement a robust framework for the efficient management and mitigation of natural hazards in terrestrial transportation modes at the Atlantic Area, which consider both road and railway infrastructure networks (multi-modal). SIRMA leads to significantly improved resilience of transportation infrastructures by developing a holistic toolset with transversal application to anticipate and mitigate the effects of extreme natural events and strong corrosion processes, including climate change-related impacts. These tools will be deployed for critical hazards that are affecting the main Atlantic corridors that is largely covered by SIRMA consortium presence and knowledge. SIRMA's objectives will address and strengthen the resilience of transportation infrastructures by:

- Developing a systematic methodology for risk-based prevention and management (procedures for inspection, diagnosis and assessment);
- Implementing a decision-making algorithm for a better risk management;
- Creating a hierarchical database (inventory data, performance predictive models, condition state indicators and decision-making tools), where information can be exchangeable between entities and across regions/countries;
- Developing a real-time process for monitoring the condition state of transportation infrastructure;
- Enhancing the interoperability of information systems in the Atlantic Area, by taking account of data normalization and specificity of each country.

Document Information

Document Name	Remote Sensing in Mapping & Inspection	
Version No.	V1.0	
Due date	31/10/2020	
Report date	06/11/2020	
Number of pages	60	
Lead Author	Pablo del Río (Uvigo); Ana Novo (Uvigo); Ana Sánchez (Uvigo); Ignacio Rodríguez (Uvigo)	
Other Authors	Joaquín Martínez (Uvigo) Belén Riveiro (Uvigo)	
Dissemination level	Confidential	

Document History

Ver.	Date	Description	Authors	Checked by
0.1	16/08/2020	Creation of the document	Belén Riveiro, UVigo	Joaquín Martínez
0.2	30/10/2020	Content input	Pedro Arias, Henrique Lorenzo, Manuel Cabaleiro, Borja Conde, J.Carlos Caamaño, Ana Sánchez, Luis M. González	Belén Riveiro, Joaquín Martínez
1.0	06/11/2020	Final formatting	Ana Sánchez, Uvigo	Belén Riveiro

Document Approval

Ver.	Name	Position in project	Beneficiary	Date	Visa
1.0					

Executive Summary

The aim of this document is to present the remote sensing platforms to be used for data acquisition in the context of SIRMA project. Moreover, a general view of the monitoring scenarios is also exposed.

The inspection of the road and railway network will be performed considering their division in two main groups: the structure of the infrastructure and its surroundings. The remote monitoring technologies are: (i) laser scanning, (ii) photogrammetry, and (iii) satellite imaging.

Operators and infrastructure owners presented some requirements that should be met by the specific technologies that will be used in each of the case studies of SIRMA. Based on the user needs, the monitoring scenarios can be defined, and data acquisition protocols can be addressed.

Table of Contents

1. Introduction and Context

This document offers a detailed description of the remote sensing platforms to be used for data acquisition of road and railway networks in the Atlantic Area.

SIRMA aims to develop, validate and implement a robust framework for the efficient management and mitigation of natural hazards in terrestrial transportation modes at the Atlantic Area, which consider both road and railway infrastructure networks (multi-modal). SIRMA leads to significantly improved resilience of transportation infrastructures by developing a holistic toolset with transversal application to anticipate and mitigate the effects of extreme natural events and strong corrosion processes, including climate change-related impacts. These tools will be deployed for critical hazards that are affecting the main Atlantic corridors that is largely covered by SIRMA consortium presence and knowledge. SIRMA's objectives will address and strengthen the resilience of transportation infrastructures by:

- Developing a systematic methodology for risk-based prevention and management (procedures for inspection, diagnosis and assessment);
- Implementing a decision-making algorithm for a better risk management;
- Creating a hierarchical database (inventory data, performance predictive models, condition state indicators and decision-making tools), where information can be exchangeable between entities and across regions/countries;
- Developing a real-time process for monitoring the condition state of transportation infrastructure;
- Enhancing the interoperability of information systems in the Atlantic Area, by taking account of data normalization and specificity of each country.

In order to fulfil this, the project proposes to use different remote sensing technologies in order to collect the necessary data to perform infrastructure monitoring. The monitoring techniques to be used in SIRMA project are divided in two main groups: terrestrial monitoring and satellite monitoring. Terrestrial remote sensing technologies use LiDAR sensors and image-based sensors to obtain geometric and radiometric data from the scenarios under study with high resolution and accuracy. On the other hand, satellites might be equipped with radar or optical sensors, monitoring a wide area as images for monitoring the real state of the infrastructure and its surrounding area. Depending on the specific application, one technology or other will be used in SIRMA. The selection will be made taking into account the requirements and fulfilling the necessities of the infrastructure owners and their operators.

With this context, this document contains the following information:

- State of the art review on remote sensing technologies for monitoring transport infrastructures. Current trend on remote sensing-based applications (Section 2)
- Background in remote sensing technologies and platforms to be used in the context of the project (Section 3)
- Description of the monitoring scenarios chosen in the Atlantic Area (Section 4)
- Dara acquisition protocols for the monitoring of critical infrastructures (Section 5)

2. State of the Art in Remote Sensing for the Monitoring of Transport Infrastructure

This section presents the state-of-the-art concerning the monitoring of the transport network, both road and railway infrastructures, using remote sensing technologies. The focus is put in the latest trends on applications and data processing practises.

2.1 Inspection and Monitoring of Road networks

2.1.1 Terrestrial monitoring

LiDAR technologies, and specifically mobile mapping systems (MMS) including LiDAR, allow to rapidly and comprehensively collect information of the road structure, its features and assets from its environment in form of point cloud data, which can be enriched with images. Continuous advancements in computer technologies have made possible the progressive automation of data processing for three-dimensional (3D) point clouds.

2.1.1.1 Surface extraction

One of the first steps that is usually taken within the workflow of a road point cloud analysis is to segment the road itself (i.e. the road surface) from the rest of the objects captured in the point cloud. There are different approaches to carry out this task. Some of them are based on an initial conversion of the point cloud into a two-dimensional (2D) raster image, projecting the 3D points onto a plane, so image processing methods can be applied to extract the ground. In (Rodríguez-Cuenca et al., 2016), the captured 3D data is projected onto the XY plane to apply a segmentation algorithm. This algorithm is based on morphological operations, detecting curb edges using the roughness data contained in the point cloud. Another computer vision technique that can be applied for road segmentation on a raster is the use of parametric active contour models (also called “snake models”). This consists on getting a parametrized curve to adapt it to an object boundary by balancing an energy function, which is useful to extract the road edges and therefore, delimitate the road surface area. (Kumar et al., 2013) combined two of these models, namely GVF (Gradient Vector Flow) and Cohen’s balloon model, to define an algorithm capable of extracting road edges from point cloud data (elevation, reflectance and pulse width); they also introduce a novel initialization of the snake model based on the trajectory information from the mobile mapping system.

The surface extraction process can also be done directly from 3D data, using voxelization techniques instead of rasterization. In (Zai et al., 2018), the point cloud is divided in several blocks to simplify its processing, and then facets (supervoxels) are generated according to the points’ attributes, integrating neighbouring coplanar points. Boundary points between non-coplanar facets are extracted, selecting those corresponding to road edges according to the trajectory data of the surveying vehicle. Road boundaries are generated through energy minimization, using an iterative graph-cuts based algorithm.

Another way of detecting road boundaries for road segmentation is by analysing the inherent geometric information from unorganized point clouds, as presented in (H. Wang et al., 2015).

In this work, the road is partitioned based on the vehicle trajectory and then, a saliency analysis is conducted to separate points in two groups: one for points belonging to vertical surfaces, and other for horizontal surfaces. Salient points are filtered to detect potential curb points, based on their elevation, horizontal length and distance to the trajectory. A modified version of this method is presented in (M. Soilán et al., 2018) to detect accessible road entrances for pedestrians by analysing the extracted curb points and comparing the entrance coordinates with pedestrian crossings locations.

2.1.1.2 Road markings

Detection of road markings is a basic task to evaluate the condition of roads, as assessing the visibility and wear state of the markings is crucial for the safety of drivers and other users of the road. Road markings detection is also a requisite for enabling autonomous driving vehicles. Detection and recognition techniques rely on photographic images or video frames as inputs to a large extent. In (Ding et al., 2019), road areas containing marking are detected on video frames by finding the vanishing point (i.e. the "converge point of a set of parallel lines in the projected transformation of a recorded 3D scene"). Then, an IPM (Inverse Perspective Mapping) transformation is applied using information about the camera pose to remove the perspective deformation effect. This produces a bird's eye image that improves efficiency for marking detection and tracking through the video record, which is performed via MSER (Maximally Stable Extremal Regions). MSER is also used by (Jia et al., 2018) to detect road markings, although in this case a biologically visual perceptual model is chosen to extract marking candidates, obtaining their sparse representation. These sparse solutions are combined into a training set to train an AdaBoost (Adaptive Boosting) machine learning classifier for markings.

In order to detect markings on the road surface from point clouds, a typical approach is to conduct a rasterization of the road, once segmented, to create an intensity image; this is, an image where each pixel represents the intensity information of the 3D points projected on that pixel. Because intensity is a measure of the reflectivity, points from road markings will show a different intensity compared to those from the rest of the pavement. In (B. Riveiro et al., 2015), image processing algorithms are used to isolate painted areas of the raster image via a binarization process based on the Otsu thresholding method; then, a median filtering is applied to remove noise and gaps on marks' borders are filled with a closing operation. Zebra crossings are detected within the painted areas with a Standard Hough Transform and considering logical constraints. The same technique is employed in (Arias et al., 2015).

In (Mario Soilán et al., 2017), once the markings are extracted from the intensity image and further processed to increase their quality, a feature vector GBF (Geometry-Based Feature) is generated for each image of a single road marking, containing information about area, shape and pixel distribution of the image. These feature vectors are fed into a supervised machine learning algorithm that classifies each marking into three possible types: rectangular markings, arrows, and others/negatives. In a second hierarchy level of the classification, a semantic meaning is assigned to rectangular and arrow markings.

2.1.1.3 Road cracks

Machine learning is also used to detect road cracks on images. A supervised deep Convolutional Neural Network (CNN) is introduced in (I. Zhang et al., 2016) to this end. It is able to provide a probability map for an image, determining for each point in the image if it corresponds to the crack or to the background. The use of a CNN to provide probability maps for crack detection from images is also explored in (Kim & Cho, 2018), using transfer learning to take advantage of AlexNet for such a task.

Cracks can also be detected within a 3D point cloud by analysing singular features of the points belonging to cracks. Crack points usually show lower intensity values compared to those on their surroundings, as stated in (Y. Yu et al., 2014), in which the Otsu thresholding method is used to select crack candidates. Outliers within the candidates are removed with a spatial density filter, as they tend to be dispersedly and irregularly distributed. An algorithm based on L1-median is used to generate 3D skeletons representing the geometric structures of crack-lines. Alternatively, (X. Chen & Li, 2016) proposed the analysis of local elevation jumps embedded in the 3D points to detect cracks. This was done applying a high-pass filter to a DTM (Digital Terrain Model) raster image to distinguish those elevation changes.

Another approach for road cracks extraction consists of first generating a geo-referenced feature image (GRF image). In (Guan, Li, et al., 2015), the ITVCrack method is introduced, consisting on extracting cracks from a noisy GRF image based on the intensity feature via Iterative Tensor Voting.

2.1.1.4 Manhole covers

Manhole covers can be detected following different approaches, some of which are directly related to the techniques detailed above to detect other road elements, like road markings or cracks, via feature analysis. (Yongtao Yu et al., 2015) proposed the use of supervised machine learning to extract high-order features from a GRF intensity image, and a random forest model to learn the probability of appearance of manholes. Both methods combined lead to the extraction of manholes.

2.1.1.5 Traffic signs

As it is the case for road markings, traffic sign detection and recognition (TSD and TSR, respectively) is essential for road monitoring, as well as indispensable for autonomous driving. Nowadays, the use of computer vision techniques based on machine learning to detect and recognize traffic signs on images is widely extended. A convolutional neural network is used in (Jain et al., 2019) as a TSR, adjusting the hyperparameters of the network (namely the learning rate and the number of epochs for each layer) via a genetic algorithm and a variation of the later involving “ternary crossover operator”. Other machine learning classifiers, such as SVM (Support Vector Machine), ELM (Extreme Learning Machine) and k-NN (k-Nearest Neighbour) are used for traffic sign recognition in (Gudigar et al., 2019).

Regarding the detection and classification of traffic signs from point clouds, both radiometric and geometric features of points are considered. This approach is followed in (Belén Riveiro et al., 2016), starting with the creation of an intensity map through rasterization that first coarsely outlines the brightest points of the point cloud, to follow with an optimized threshold

that isolates points belonging to traffic signs, which are clustered together and each sign is then classified according to its function.

3D point clouds can be combined with 2D images to increase the semantic information of extracted traffic signs, as it is demonstrated in (Mario Soilán et al., 2016) by retro-projecting the 3D positions of traffic signs on 2D images captured by RGB cameras. Machine learning image analysis techniques can then be applied to recognize traffic sign semantics and classify them.

2.1.1.6 Pole-like objects

There are other objects placed along roadsides that, just as traffic signs, have singular morphologies that allow to separate them from the rest of the point cloud. In (Yan et al., 2017) pole-like objects, like traffic lamps, are detected in point clouds (after ground segmentation) based on previous knowledge and shape information, and classified with Random Forest. Furthermore, (Cabo et al., 2014) introduced a method to first carry out a voxelization of the point cloud to regularize it and increase computer performance, and then identify pole-like objects through a 2D analysis of the horizonal section of the voxelized cloud.

2.1.1.7 Trees

Trees are other type of significant roadside objects to be extracted from point clouds. Their non-photosynthetic elements (i.e. trunk and branches) can be clustered together by combining points with methods like the one introduced in (Xu et al., 2018), minimizing an energy function based on Euclidean distance. Another example of clustering based on Euclidean distance is presented in (Guan, Yu, et al., 2015), in which PCA (principal component analysis) is used to describe the local point distribution of extracted off-road objects. Then, feature vectors are produced for each object classified as tree/non-tree with a SVM algorithm.

2.1.1.8 Infrastructure information models

These methods to analyse the road and its assets can be integrated in a framework to produce an infrastructure information model, namely a BIM (Building Information Modelling) model for infrastructure. In (Mario Soilán et al., 2020), a methodology to process point cloud data is presented. This includes ground segmentation, road marking detection and extraction, and road edge detection, to output an IFC (Industry Foundation Classes) file that models the road alignment as well as the centreline of each lane. The point clouds are processed in a semi-automated manner, combining automatic processing and manual validation. The generated files are compliant with the IFC4.3 schema specification from buildingSMART.

2.1.1.9 Forest monitoring

Forest fires are an immense burden to the environment, infrastructure, economy, and most importantly, human life around the world. Fires are considered as a significant environmental issue because they cause prominent economic and ecological damage. Fire behaviour is highly conditioned by vegetation characteristics, and particularly by the amount and spatial distribution of fuels. Roads are a key element in forest fire fighting, providing both access to wildfires during extinguishing tasks and acting as linear firebreaks that avoid or reduce fire spread. These factors can be useful in both fire suppression and prescribed fire operations. Nevertheless, the benefits that roads provide for fire prevention and fire management carry

an associated maintenance cost (Gucinski et al., 2001). Human-caused fires are initiated by accidents, negligence, or arson. Road access is a significant contributing factor in the occurrence of this human-caused ignitions (Freden et al., 1974). The 70% of forest fire occurred close to main roads, within 500 m of them (Ganteaume et al., 2013). The increased ignition risk related to increasing housing and road density may be additionally modulated by the vegetation types crossed by roads (Freden et al., 1974).

Data mining applications such as convolutional neural network, fuzzy metaheuristic ensembles, genetic algorithms, etc. became popular for setting optimal combination of forest fire related variables, and modelling forest fire susceptibilities (Hong et al., 2018). (Chamoso et al., 2018) proposed that UAVs can be used in fire control due to their ability to manoeuvre rapidly and their wide range of operation. Fire detection techniques using computer and infrared computer techniques, as well as the hardware systems that drones must be incorporated to perform this task. (Sherstjuk et al., 2018) have worked upon tactical forest fire-fighting operations based on a team of UAV and remote sensing and image processing techniques.

LiDAR is another common remote sensing technology applied in forestry studies. Although a variety of technologies can be used to spatially describe forest biomass distribution, active sensors such as Terrestrial Laser Scanning (TLS) (Pimont et al., 2015) and Airborne Laser Scanning (ALS) has been proved very useful to characterize the 3D forest structure (García et al., 2018; Yunsheng Wang et al., 2016). However, the interception of the laser beam by the upper canopy strata may impede accurate understory strata assessment with ALS (Hamraz et al., 2017; Kükenbrink et al., 2017). Airborne laser scanning based on unmanned aircraft systems has an excellent tree height measurement performance, mobility, and fast data acquisition, which make it a very attractive option for forest investigations (Liang et al., 2019). The fusion of LiDAR data and spectral imagery has been used to address the limitation of only using LiDAR data in vegetation mapping (Su et al., 2016).

Recent advancements in remote sensing technology have facilitated new approaches to studying fire ecology. Of particular interest for fire managers, LiDAR has been incorporated into the mapping of fuels (García et al., 2011), assessing burn severity (Kane et al., 2014), and monitoring vegetation recovery (Gordon et al., 2017).

2.1.2 Satellite monitoring

Since the Copernicus Sentinel-1A launch on 8th April 2018, the publication of works regarding infrastructure monitoring started to increase. Interferometric Synthetic Aperture Radars (InSAR) are consolidating as a valid tool to observe deformations on the earth's surface; this is because the data is supplied for free in different platforms compared with the rest of satellites for commercial use. In addition, Sentinel-1A also supposes an evolution compared the past Band-C European missions based on the synthetic aperture radar system (SAR), which were the European Remote Sensing Satellite (ERS) and the Environmental Satellite (ENVISAT). This evolution, apart from improving technology in the sensors, supposes the reduction of the temporary review time from 35 to 6 days. With this, images can be obtained with more frequency to detect changes on the earth's surface, and to make a more effective and reliable

monitoring. In this way, a large number of works demonstrated good results for performing infrastructure and forest monitoring.

2.1.2.1 Infrastructure monitoring

One of the main applications of satellite data for infrastructure monitoring is the measurement of subsidence. In (Delgado Blasco et al., 2019), the measurement of the urban subsidence in the Rome metropolitan area was carried out (Figure 1). This work uses the method of Multi-temporal Interferometric Synthetic Aperture Radar (MT-InSAR), which consists of comparing a time series of the different interferometric images of the radar. The deformations existing in the highway network of the Rome metropolitan area are obtained as the differences between images. Deformations are measured with millimetre accuracy (from –10 mm to +2 mm). These results are obtained through the SNAP-StaMPS program using the Persistent Scatterer interferometry (PSI) technique, which consists on the analysis of pixels that remain consistent over the sequence of interferograms.

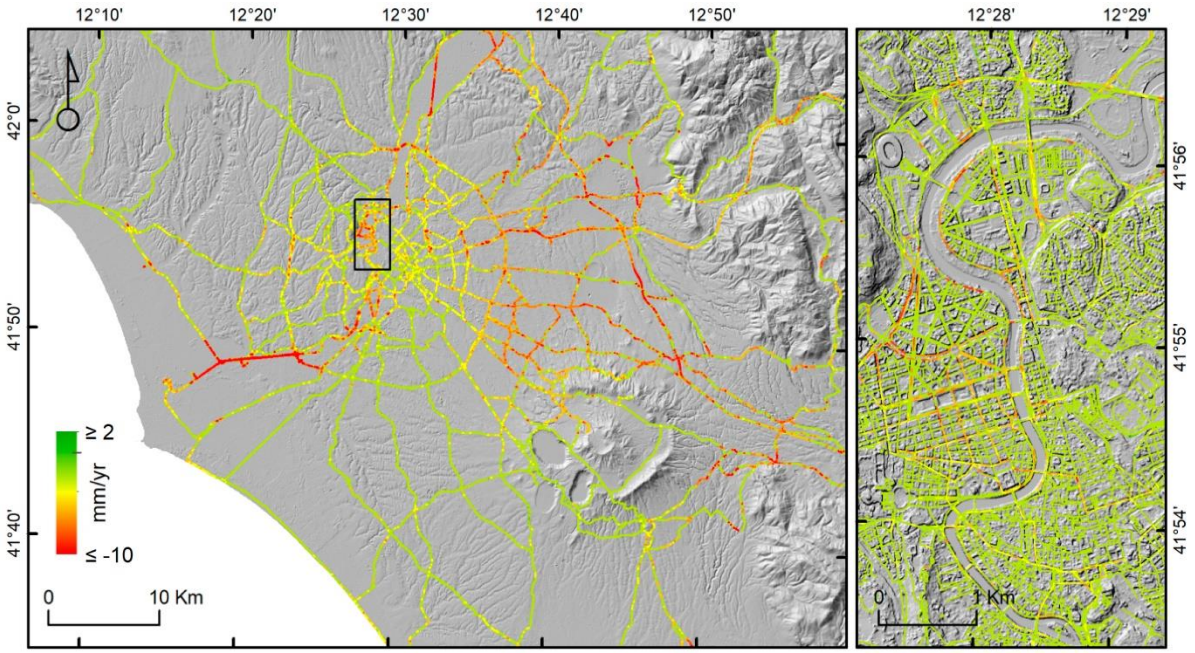

Figure 1: Average vertical movement rates along motorways, primary and secondary road networks (left); and detail of the city of Rome including tertiary, residential and pedestrian roads (right) (Delgado Blasco et al., 2019)

2.1.2.2 Forest monitoring

The use of remote sensing techniques to study the forest fire area is a useful way of providing information before, during or after a fire. Regarding pre-fire information, the possible applications are: fuel type mapping, fire risk evaluation, and beginning determination of danger period, among others. During a fire, the information that can be provided by remote sensing systems refers mainly to the location of active sources through the use of thermal sensors. Finally, post-fire information can refer to affected surface evaluation and the monitoring of burned areas over time.

The most used remote sensing systems for fire ecology research are space-based multispectral sensors. Imaging data has become a primary data source for forest fire mapping and

monitoring in inaccessible forest regions (Xiao-rui et al., 2005). Because of the requirement of high temporal resolution in case of forest fires, the Moderate Resolution Imaging Spectroradiometer (MODIS) data are often a primary choice owing to their daily repetitive coverage and ability to detect fires in remote regions. On the other hand, the risk to forest fire is estimated based on meteorological data or from vegetation indices. The satellite-based evapotranspiration rates are a good estimate of fire risk assessment (Vidal et al., 1994). Satellite sensors such as SPOT, Landsat TM/ETM and OLI, AVHRR, ERS2, RADARSAT, etc. have been used to map the burned areas, change detection, damage, and risk assessment. Yuan et al. (Yuan et al., 2017) recently presented the applicability of UAV mounted infrared (IR) imaging systems for the automatic detection of fires in forest regions. Vegetation indexes including Normalized Difference Index (NDVI), Green Normalized Difference Vegetation Index (GNDVI), Normalized Burn Ratio (NBR), and Normalized Difference Vegetation Index (NDVIreXn) that implements red edge spectral bands showed high competence in mapping post-fire scenarios (Navarro et al., 2017).

2.2 Inspection and Monitoring of Rail networks

2.2.1 Terrestrial monitoring

The monitoring of the railway network, as for the road network, may be done using different remote sensing technologies. Although the use of diverse sources of data like RGB cameras, thermographic cameras or radar, could be also considered in this section, there are few works to this regard. Laser scanning is then presented as the head technology to monitor the railway infrastructure. Moreover, it is one of the best technologies to gather exhaustive information of the railway line.

As explained subsequently in Section 3.1.1, there are three types of laser scanning systems: terrestrial laser scanners (TLS), mobile laser scanners (MLS) and aerial laser scanners (ALS). Depending on the application, the logic is to use a different system. Even though there are some works regarding the use of ALS and TLS data for monitoring the railway network, it seems appropriate to use MLS since these devices can collect large amounts of data in a short period of time and with high resolution. Taking this into consideration, this section is in charge of making a summary of the main applications of mobile laser scanning in the railway network.

2.2.1.1 Railway inventory

Laser scanning is considered one of the best non-destructive techniques (NDT) for the gathering of information regarding the as-is state of the environment. One of its main applications in the railway environment is the inventory of the infrastructure elements. One of the most recent reviews to this respect is the one presented by (Che et al., 2019), where MLS data were used for object recognition and the extraction of their characteristics.

Continuing with classification methods, several works from the author Arastounia, M. are meaningful when talking about heuristic methodologies for inventory purposes in the railway environment (Arastounia, 2012, 2015, 2017; Arastounia & Elberink, 2016). In this line of research and inspired on these works, (A. Sánchez-Rodríguez et al., 2018) created a method for the automatic labelling of railway tunnel point clouds from MLS data. There are also several

works regarding the classification of railway point clouds but helped by specific programs for post-processing the point clouds under study (Al-Bayari, 2019; Leslar et al., 2010).

In the recent years, the use of deep learning algorithms with classification ends has been increasing. An example of this is the work of (Rizaldy et al., 2018), where ALS data are used as input of Fully Convolutional Neural Networks in order to classify ground points. Regarding the work with MLS data, (M. Soilán et al., 2020) proposed algorithms for the automatic segmentation of point clouds using PointNet and KPConv newural networks, but applied in this case to railway tunnels. They use the resulting labels of an heuristic classification method (A. Sánchez-Rodríguez et al., 2018) for training the aforementioned neural networks.

Another rising application is the creation of three-dimensional (3D) models utilising point cloud processed data. The use of Digital Twinning and BIM (Building Information Modelling) has been evolving in the recent years. They have grown from their exclusive use for buildings to its application for large infrastructures (Nuttens et al., 2018). To this regard, (Cheng et al., 2019) developed a method for the generation of as-is BIM models of railway tunnels using TLS data. First, they applied classification algorithms to the point cloud, and then, they estimated the modelling parameters in order to create the BIM model. There are more works regarding the creation of three dimensional models from LiDAR data, but they are focused on specific elements of the railway environment. These are to be described subsequently.

2.2.1.2 Rail tracks

One of the most common applications of railway point clouds is the extraction of the rail centreline. This information allows to make a good estimation of the location of the railway network and its fusion with GIS maps. There are several publications in this field of research, working with both ALS and MLS data (Beger et al., 2011; Elberink & Khoshelham, 2015).

Another important application is the detection of rail tracks. Publications in this regard are more common since the inspection of these elements is very common when working with laser scanning data, as reflected in Section 2.2.1.5. (Lou et al., 2018) proposed a workflow for rail track detection using MLS data from a low cost LiDAR sensor. The methodology is based on their physical shape, geometrical properties and reflection intensity values. This work is also relevant as it is supposed to process data in real time. In addition, the work developed by (Ana Sánchez-Rodríguez et al., 2018) also classifies rail track points from MLS data combining the application of heuristic methods with an automatic classifier (SVM, support vector machine).

The creation of 3D models of rail tracks from railway point clouds it is not a new trend (Soni et al., 2014; Yang & Fang, 2014)). (Hackel et al., 2015) developed a methodology for the classification of rail track points (among others) using template matching algorithms. This methodology has proved good results working with data from any laser scanning system.

Detecting and modelling rails from MLS data based on the properties of the tracks and contact wires. The main step for detecting rail track points is to fit a parametric model to them. After other processing steps, a mesh model is created (Oude Elberink et al., 2013).

2.2.1.3 Power line

The inspection of the power line in the railway network is essential for the good functioning of the service. Before performing inspection tasks in these elements, it is necessary to first detect them in the point cloud. One of the main algorithms used to classify power line points is RANSAC (RANdom SAmple Consensus) (Fischler & Bolles, 1981). Several authors use this statistical method to group cable and catenary points (B. Guo et al., 2016; Jeon & Choi, 2013; Pastucha, 2016). A recent work presented by (Ana Sánchez-Rodríguez et al., 2019) showed good results when applying this method in railway tunnel point clouds.

To this respect, (Cserép & Mayer, 2020) made a review of the recent trends when detecting power line cables. Then, they propose a method for the classification of power line points using a smaller point cloud as seed for growing from the full one. It uses RANSAC and region growing, among other algorithms, to label points. Another example of the use of region growing algorithms for classifying catenary points was developed by (S. Zhang et al., 2016), proposing a self-adaptative growing algorithm. Continuing with the analysis of connectivity between points, (Yanjun Wang et al., 2018) presented a workflow where they also used the Hough transform for grouping purposes.

Working with machine learning tools, (Jung et al., 2016) proposed a method for locally classifying points using support vector machines. Ten classes were obtained, representing each of the elements of the overhead wires. A step forward is given by using deep learning algorithms with the same aim. A recent work presented by (Corongiu et al., 2020) proves the validity of these algorithms for the classification of railway cantilevers and portal masts. Their work is based on a mixed approach: firstly, they select specific areas based on PCA (principal component analysis) results (Jolliffe, 1986). Then, a 3D-modified Fished vector-deep learning neural net is used to classify candidates.

Regarding the work with imaging data, (Fu et al., 2018) developed a method for the extraction of geometric parameters of the power line to be used as input for the 3D modelling of the infrastructure. Continuing with the generation of digital models of the infrastructure, (Ariyachandra & Brilakis, 2020b) proposed a novel method for the generation of digital twins of the overhead line equipment of railways from ALS data. They restricted the search of wire points relative to railway masts detected with a previously developed algorithm (Ariyachandra & Brilakis, 2020a), and then converged the resulting power line cable clusters with different parametric models to obtain the digital twins.

2.2.1.4 Signalization

The use of point clouds for the automatic classification of signalization points has not been explored a lot. It is expected that in the coming years, the interest in this point labelling will start to arise, as there is a lot of work already developed thanks to the road monitoring (Section 2.1.1). Nonetheless, it is worth mentioning the work from (Karagiannis et al., 2020), where a method for sign detection is proposed but using RBG or video images. The classification is performed using a Faster R-CNN (Convolutional Neural Network for object detection).

2.2.1.5 Inspection

The monitoring and inspection of the railway line using non-destructive techniques has been rising in the recent years, although this is not new. (Zarembski et al., 2014) already presented a review of several key track substructure inspection technologies, including the traditional ones and also new ones like LiDAR or ground penetrating radar. It is also highlightable the application of thermographic cameras for monitoring (Minbashi et al., 2016). A more recent review published to this respect is the one by (Falamarzi et al., 2019), where the main techniques used to detect damage in railway environments are presented. And later on, (Artagan et al., 2020) exposed the most recent NDT for health monitoring of railway infrastructures.

With respect to the use of laser scanning as an NDT for monitoring the railway infrastructure, there is not a defined technique to perform this, but some works have been developed to this end. The most common elements to be inspected are rail tracks. A methodology using CAD models to compare with LiDAR data for rail wear measurements was presented by (P. Chen et al., 2017). Continuing with rails condition, (Taheri Andani et al., 2018) proposed the detection of different rail surface conditions using indices defined based on LiDAR data. In this direction, (Sadeghi et al., 2019) proposed an index for ballast inspection using automated measurement systems.

Some methodologies have also been proposed for clearance monitoring. (Mikrut et al., 2016) used MLS data to create a 2D image of different cross sections so that an operator could detect suspicious areas. In addition, the work from (Niina et al., 2018) is also significant for visually checking the clearance on point clouds. More recently, (Ana Sánchez-Rodríguez et al., 2019) proposed a workflow not only for classifying power line points (Section 2.2.1.3) but also for its automated inspection on tunnel point clouds, measuring clearance gauge and deflection of the catenary cables. Continuing with tunnel point clouds, an algorithm for the monitoring of tunnel deformation using TLS data was developed by (Xie & Lu, 2017). They pre-processed the point cloud to generate a 3D model of the tunnel and measurements where performed on it.

2.2.1.6 Forest monitoring

Wildfire ignition risk increases as the density of urban, road or railway developments do (Vilar et al., 2010). Vegetation becomes combustible and the risk of fire increases during periods of hot weather. Fires can damage the railway infrastructure and railway authorities are very much concerned (Nyberg et al., 2013). This is due to lack of knowledge concerning the status of vegetation on and alongside railway embankments. Hence, periodic maintenance actions (e.g. inspections, mechanical harvesting, spraying herbicides, etc.) are employed for controlling vegetation.

Manually inspecting vegetation is very a slow and time consuming process, and maintaining an even quality standard is also very difficult. An alternative is to use new technologies to overcome this issue. The machine vision approach has performed reasonably well for detecting the presence of vegetation on railway tracks when compared with a human operator (Yella et al., 2013). (Hulin & Schussler, 2005) presented a mounted system based on three multi-spectral cameras on a train to generate a vegetation profile and register vegetation for efficient vegetation management. There are few recent studies on vegetation

detection around railways (Matson et al., 2018; Nyberg, 2016; Yella & Nyberg, 2016). Similarly, the road and railway have the same consideration regarding wildfires occurrences (Conedera et al., 2015; F. Guo et al., 2016; Molina et al., 2019; Serra et al., 2014).

2.2.2 Satellite monitoring

There are not many research works regarding the use of satellite data for monitoring railway infrastructure. Nonetheless, (Chang et al., 2017) presented one study of the deformation of the Dutch railway network using one stack of C-band SAR images from the satellite Radarsat-2. The images were acquired between June and August 2015, the repetition frequency of the satellite was 24 days. They analysed a total of 213 images, obtaining deformation values from ± 10 mm per year; in which 4 interest areas with higher deformation values stand out. These deformations were analysed in more detail, getting as possible explanation the type of soil (hydromorphic soils) supporting these railway lines.

2.3 Inspection and Monitoring of critical structures

One example of monitoring of critical structures is the detection of dam subsidence. The Three Gorges Dam analysis (Z. Wang & Perissin, 2012), is a demonstration of the possibilities that the use of remote sensing presents using Cosmo SkyMed stripmap images from February to August 2011. The authors managed to verify the deformation that occurs in the dam with SARPROZ commercial software.

Another applicable example of monitoring is for the case of specific buildings. (Bakon et al., 2014) made a study of the city of Bratislava using also SARPROZ software and the ENVISAT satellite (Figure 2). With this, a deformation rate of -20 mm of the building was obtained, caused by one neighbouring construction. These results were obtained by applying the persistent scatterer interferometry technique (PSInSAR).

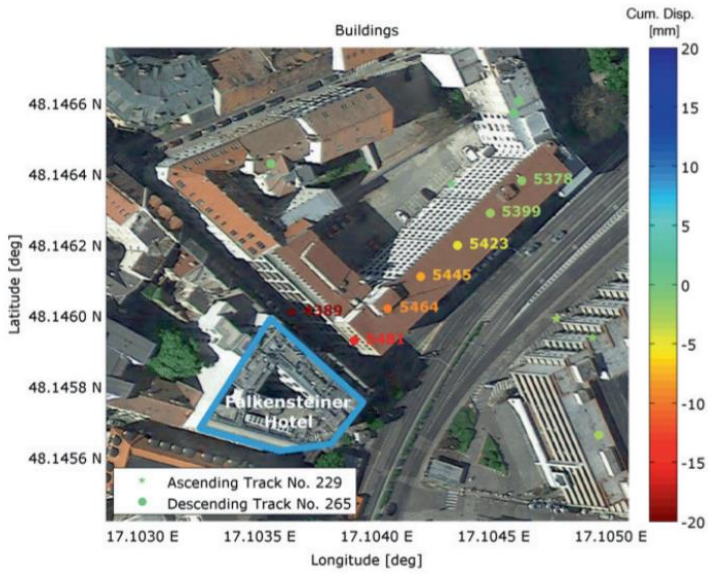

Figure 2: Building affected by the excavation trench of a nearby hotel, September 2007 (Bakon et al., 2014)

Lastly, it its highlightable the study about the collapse of the Hintze Ribeiro bridge on 4th March 2001, in Portugal (Sousa & Bastos, 2013). It is a perfect example of the monitoring of critical structures, since it detects the movements produced before the collapse of the bridge (Figure 3). In order to achieve this, the authors use the SNAP-StaMPS software combining the PSInSAR and the small baseline subsets (SBAS) techniques. This last technique is based on making a series of combinations of pairs of SAR images, which are characterized by having the lowest possible orbital separation, in order to generate a series of interferograms with low spatial decorrelation. They used 52 images obtained by the ERS -1/2 satellites between the period of May 1955 and December 2000. The deformation rate is quite considerable because the maximum velocity detected is approximately 20 mm per year, precisely in the structure of the collapsed bridge. This analysis confirms the capacity of the MTI techniques for the monitoring of deformations, even using a low resolution satellite like ERS.

Therefore, it is confirmed that the continuous processing of the InSAR observation could be successfully integrated into infrastructure monitoring programs in the implementation of early warning systems.

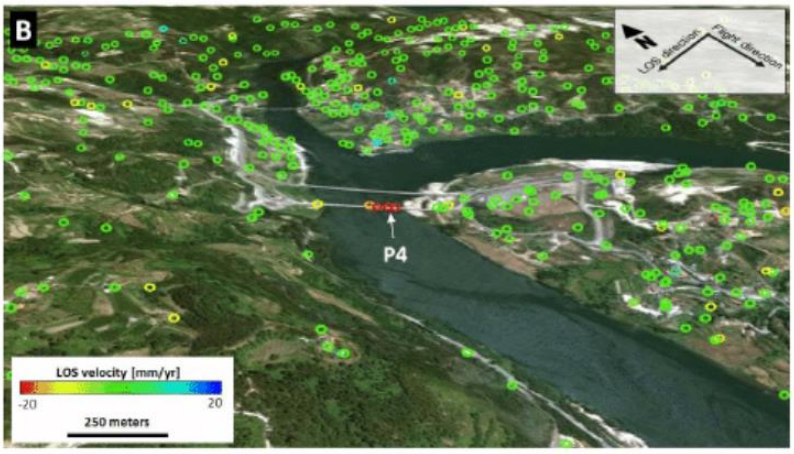

Figure 3: Color-coded average linear deformation rate overlaid on a Google Earth image with the collapsed pillar highlighted (P4). The observation geometry is indicated in the upper right corner. Figure generated by viStaMPS (Sousa & Bastos, 2013)

3. Background in Remote Sensing and technologies

3.1 Remote Sensing Technologies

3.1.1 Laser scanning systems

3.1.1.1 LiDAR sensors

A LiDAR (Light Detection And Ranging) is a type of sensor that is capable of measuring distance by emitting laser beams that impact on an objective and bounce back to a receiver. To obtain the distance measurement, also known as range, it is necessary to infer it by either registering the time that it takes to a backscatter of the laser beam to return (i.e. Time-of-Flight or ToF) or the phase difference between the emitted and the received signal, a technique that is known as continuous wave (CW) modulation. The amplitude of the returned laser signal allows

to calculate its intensity, which is related to the reflective properties of the surface of an impacted object. Some receivers are as well able to collect multiple echoes from a same emitted beam, which often occurs if the impacted object is translucent/transparent or disperse (like canopy of trees).

Typical LiDAR sensors are capable of emitting hundreds of thousands of laser beams per second, registering a point every time the laser impacts an objective, which is referenced based on the measured distance and the instantaneous orientation of the sensor. Therefore, they have the capacity to scan the environment rapidly and with great resolution. To measure distances in different directions, a LiDAR sensor needs to be able to change its orientation, so it is mounted onto an opto-mechanical assembly based on a spinning mirror that deflects the laser beam in 360°. Furthermore, making the sensor rotate around an axis perpendicular to that of the spinning mirror, is possible to guide the laser beam in every direction of the 3D space, describing a sphere around it. This is the case for TLS (terrestrial laser scanning) sensors, which remain fixed in the same position during the whole acquisition process, while MLS (mobile laser scanning) systems usually obtain multiple 360° scans along the trajectory of the vehicle in which they are mounted on. ALS (aerial laser scanning) systems create scans of the ground by combining their movement with different sweeping patterns. The set of registered points in 3D coordinates is known as a point cloud.

3.1.1.2 Positioning and navigation

In order to register the acquired point cloud to a global coordinate system, the local coordinates of the point cloud must be related to a global positioning system. Comprehensive positioning and navigation systems often combine several technologies to acquire and maintain accurate position information.

- GNSS (Global Navigation Satellite Systems) calculate their position in relation to a set of satellites within a constellation; usually 3 or 4 satellites are enough for positioning, depending on the operational mode of the GNSS. Distance between each of the satellites and the receiver is measured by estimating the propagation time of the transmitted signals. The main GNSS systems available are GPS (Global Positioning System; operated by the US Air Force), Galileo (EU) and GLONASS (Russia).
  GNSS technology count with some weak points. For instance, if the receiver is not within the line of sight of enough satellites, it would be impossible to correctly determine its position. This situation is known as an outage and is often produced in urban areas due to the amount of structures tan can obstruct the satellites' signals, or deviate them form their intended path, which is known as multipath propagation, causing erroneous distance measures.
- IMU (Inertial Measurement Unit) calculates the position and orientation of the system using accelerometers and gyroscopes, respectively. Displacement is calculated by integrating the measured acceleration into velocity and then into position and combining it with the registered orientation. As displacement is measured in relation to the starting point of the system's trajectory and thus, it does not rely on external references, the cumulative error in the estimation grows with every iteration. Because of this, IMUs are often integrated with a GNSS to introduce correction in the position

using a global reference system. In turn, as IMU reference system is internal, positioning is not interrupted during GNSS outages.

- A DMI (Distance Measurement Unit) can be mounted on a vehicle to measure its displacement by counting the rotations of a wheel and calculating the travel distance from its diameter. As an internally referenced system, like the IMU, it also accumulates error as time goes by, so it is used as a support system for the GNSS and IMU.

3.1.2 Imaging systems

A digital imaging system is a device capable of registering a scene into a digital file. The process comprises several steps. First, imaging optics focus the scene onto the image sensor, which consists of a 2D array of pixels (El Gamal & Eltoukhy, 2005). Each pixel contains a photodetector that converts the incident light into photocurrent, and readout circuits that convert the photocurrent into electric charge or voltage to read it off the array. To produce colour images, a CFA (Colour Filter Array) is placed on top of the pixel array, making each pixel to produce an electrical signal corresponding to a single colour. The light is filtered by wavelength range, giving information of the light intensity in the wavelength region of a certain colour. A common CFA configuration is the Bayer filter, a mosaic built up from 2x2 sub-mosaics with 1 red filter, 2 green and 1 blue. A micro-lens array is placed on top of the CFA array to increase the amount of light incident on each photodetector.

An Analog-to-Digital Converter (ADC) digitalizes the analogue signal read out from the pixels, so it can be processed. The full colour image is constructed from the under-sampled colour channel outputs from the CFA, via a demosaicking algorithm. Further processing includes white balancing, colour correction and mitigation of some adverse effects caused by faulty pixels and imperfect optic components. The processed image can be then compressed and stored.

3.1.3 Radar systems

Currently, remote sensing technology has evolved to achieve good results for the monitoring of infrastructures and not only for the detection of natural geohazards. This was possible by the constant private and public inversions in the satellite system developed. In this sense, the Copernicus Program supposed a true revolution in remote sensing analysis since it meant having images accessible by any citizen and any organization around the world for free, complete and open access. There are two platforms to access to the data and information services of Copernicus according to user preference: DIAS or Conventional Data Hubs. However, it is necessary to clarify that the resolution of the data offered by the Copernicus Program is not always the most suitable for infrastructures; but their free access has encouraged the development of applications to improve the usability of these images.

Copernicus Program is based on a series of satellite missions with the name of Sentinels. From 2014, these satellites provide satellite data operationally for numerous applications, including the collection of information about precision agriculture, soil movement, algae monitoring, water management, forest monitoring, climate monitoring, etc. Inside the Sentinel constellation, in the infrastructure field, the satellites used are Sentinel 1 and 2 satellite pairs.

Table 1: Characteristics of Sentinel-1 and Sentinel-2 satellites (European Space Agency, 2014, 2015)

Satellite	Data	Polarization/Bands	Launching	Resolution
Sentinel-1	Radar	VV, HH, VV+VH, HH+HV	2014 and 2016	5-20 meters
Sentinel-2	Multispectral	10 bands	2015 and 2017	10-20-60 meters

Sentinel-1 is based on Synthetic Aperture Radar (SAR) that, through the Interferometry technique (InSAR) detects deformations on surfaces comparing several images.

In order to obtain good results in the infrastructure monitoring the MT-InSAR technique (Multi-temporal Interferometric Synthetic Aperture Radar) is applied. It focuses in monitoring the deformation through the years in different epoch. For that, multiple time series of SAR images are used. With this, it is possible to reduce numerous errors such as phase decorrelation, or the error in the unwrapping of the phase and the atmospheric noises, typical of the capture and processing of the images.

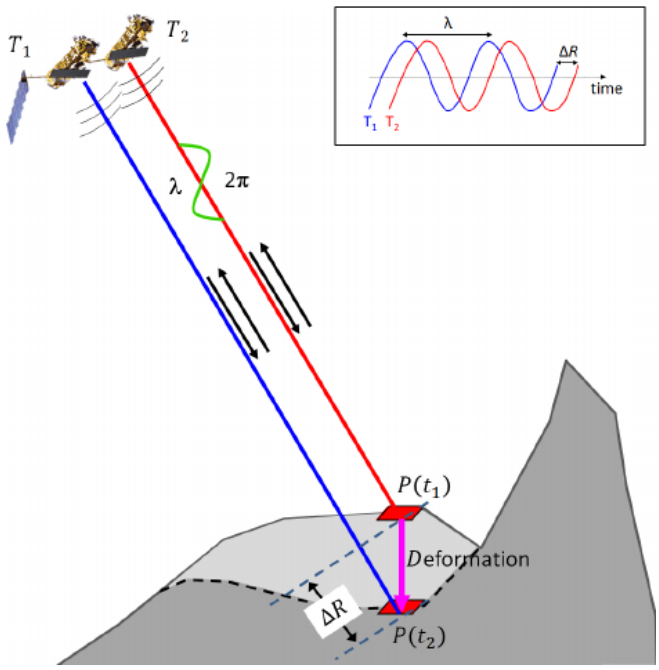

Figure 4: InSAR basic concept of comparison over time (Sousa & Bastos, 2013)

Sentinel-2 is a mission consisting of a constellation of 2 polar-orbiting multi spectral satellites for the monitoring of Earth. It provides images for vegetation, soil, water and for emergency services. It could process images by comparison and detect changes in infrastructures applying different methods and applications. These detection methods can be simple detection, normalized index change detection, and detection by supervised classification. However, in order to make a more accurate infrastructure analysis, it is necessary to use commercial images with higher resolution. For that, the use of Sentinel-1 radar data is more suitable for

infrastructure monitoring, since it is possible to have millimetre precision with the help of the specific applications oriented to these studies.

3.2 Remote Sensing Platforms

3.2.1 Land-based surveying

To perform a survey over a vast area, a mobile platform consisting of a vehicle integrating the sensors needed for the data acquisition, known as an MMS (Mobile Mapping System) is the best option. The solution to be used by SIRMA Project is the Lynx Mobile Mapper M1 platform from Optech (Teledyne Optech ©, 2019), comprising two LiDAR sensors, an integrated positioning solution (Applanix POS LV-520 IMU and two Trimble GNSS antennas) with a DMI to assist the other systems and, additionally, a Ladybug5 360° camera. This camera was installed to capture images to add semantic information to the acquired point clouds. This camera has six Sony IMX264 CMOS sensors with a resolution of 2048x2464 pixels.

Figure 5: Sensors mounted on the survey vehicle

3.2.1.1 LiDAR sensors

There are several LiDAR sensors available on the market, with different configurations, operation modes and performances. The following list includes the specifications of models from some of the most relevant manufacturers.

- Optech LYNX M1. It is the sensor model of those used in our MMS. This is a 2D LiDAR sensor based on the Time-of-Flight measuring method with 360° field of view. The scan frequency is programmable between 80 and 200 Hz, achieving a maximum PRR (Pulse Repetition Rate) of 250 kHz. It is capable of detecting up to 4 measurements from a single laser pulse. The maximum measuring range, when aiming for targets with low

reflectivity (20%) is 200 m. The range precision is 8 mm and has 5 cm of absolute accuracy.

- RIEGL VUX-1HA. It is a 2D Time-of-Flight type sensor with a 360° field of view and a scanning frequency from 10 Hz up to 250 Hz (rotations of the sensor per second). The maximum PRR of the laser is 1000 kHz, meaning that it is capable of registering 1 million points per second. It offers a maximum measuring range of 420 m for high reflective objectives working with a PRR of 300 kHz. At a 30 m range, it achieves an accuracy of 5 mm and a precision of 3 mm.
- Sick LMS 511. This model is also a 2D ToF LiDAR, with a horizontal field of view of 190° and a scanning frequency between 25 and 100 Hz. This sensor has a PRR of 19 kHz operating with a maximum range of 80 m or up to 25.5 kHz, reducing the range to 65 m.
- Velodyne Alpha Puck. This sensor operates differently, as it emits an array of laser beams (128, in the case of the Alpha model) arranged in a non-linear manner along a 40° arc. This array of lasers is rotated around the vertical axis of the device to offer a 360° field of view, being able to capture around 2.4 million points per second. The maximum measuring rate is 300 m.
- FARO Focus 350. This 3D sensor has vertical and horizontal fields of view of 300° and 360°, respectively, measuring range in 3D at a distance of up to 350 m through CW modulation. It is capable of acquiring up to 976 thousand points per second.

3.2.2 Satellite platforms

Platforms are referred to the vehicles where the sensors are placed to emit and register the electromagnetic radiation in order to capture Earth surface images. Historically, can be referred as both manned and unmanned aircraft and satellites. In this document, only the most important characteristics of the principal satellites that are currently available (both optical and radar) are to be mentioned. The difference between radar or optical satellite is that radar images are captured by active systems, this is, the satellite emits one energy beam and then catches the part that is reflected. By comparison, optical images are captured by passive systems, this is, the satellite detects the radiation that emits or reflects the object of study since the satellite has multi-spectral sensitivity. This means that it catches data from different spectral bands simultaneously. Besides, radar satellites unlike optical satellites do not depend on the atmospheric conditions; they register the data at any time, since they emit their own source of energy and do not require solar energy.

The spectral resolution of the radar images is changeable, and the capture range is not measuring in wavelengths of the electromagnetic spectrum but in frequency bands.

In radar images, the displacements of the relief happen in the opposite way instead of making the normal shadow of an optical satellite. In addition, the radar images the top parts of a structure can reflect signals before the base, inasmuch as the displacement of the relief is getting closer to the nadir instead of moving from it like the optical satellite.

In the terrain captured by the radar satellite, when the slope of the terrain is bigger than the depression angle, the radar shadows hide the characteristics in scope. Therefore, the signals from the slopes that point out the radar antenna will come back very weak. This causes dark

or black areas in the radar image, in comparison with the optical images whose main problem is the presence of clouds in order to make an effective image analysis.

Lastly, it is worth mentioning that due to the constant and high availability of data received by the platforms of different programs of the space agencies, it is important to perform calibration-validation (CAL-VAL) programs on them to guarantee the reliability of data. This CAL-VAL process starts before the launch of the platform since it is the only opportunity to directly calibrate and characterize the satellite physically. After the launch, this process indirectly continues to obtain Level 1 and 2 data reliable and calibrated. The CAL-VAL of one mission includes the sensor calibration, verification of the algorithm, geophysical data validation, and the intercomparison with other missions. All this leads to the quantification of uncertainties. This process can be improved by comparing multiple independent sources so that confidence in the veracity of the data is generated (Sterckx et al., 2020).

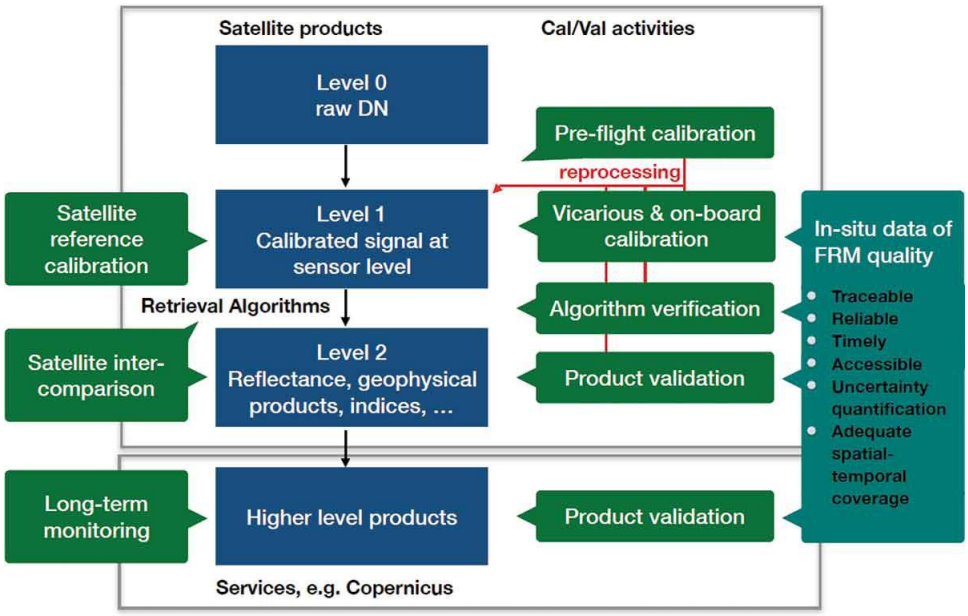

Figure 6: Representation of the necessary steps for CAL-VAL's integral activities for satellite missions on a sustained basis. Green boxes indicate specific CAL-VAL activities, blue boxes indicate steps to produce geophysical satellite data products, and red lines reprocessing activities (Sterckx et al., 2020)

3.2.2.1 Optical satellite technology

Only those satellites that are still in operation and with a very high resolution will be analysed in this section. This is because of the abundance of commercial satellites for the detection of optical images, which are key for infrastructure monitoring:

- WorldView: Consists on a satellite series for Earth observation in high resolution, with spatial resolution from 0.31 m to 5 m in panchromatic mode and 1.24 m to 1.84 m in multispectral mode with a frequency of passes not exceeding 2 days, depending on each satellite. It is a Commercial Product.
- Pléiades: It is a constellation of 2 satellites in coordinate orbit. Its principal mission is the Earth observation in high resolution, furthermore, contributes substantially in the disaster monitoring. With a frequency of passes approximate every 4 days and one spatial resolution of 0.5 m in panchromatic mode and 2 m in multispectral.

- RapidEye: It is a constellation of 5 satellites for frequent ground observation, it is a Commercial Product. With a frequency of passes approximate every 3 days and one spatial resolution of 6.5 m in multispectral.
- Satellite Pour l'Observation de la Terre: It is a 2 operative satellite series; it is a Commercial Product. For Earth observation in high resolution, furthermore, contributes substantially the disaster monitoring. With a frequency of passes approximate every 4 days and one spatial resolution of 1.5 m in panchromatic mode and 6 m in multispectral.
- Deimos: Consists in a satellite series for Earth observation. It is a Commercial Product. With a frequency of passes approximate every 2 days and one spatial resolution of 0.75 m in panchromatic mode and 4 m in multispectral.

The constellation of Sentinel-2 is a platform that provides free, systematic and open data. Its main mission is the land and vegetation observation. The Copernicus Sentinel-2 is a constellation of two satellites, Sentinel-2A and Sentinel-2B. They are in polar orbit placed in the same synchronous orbit with the sun, in phases of 180° from each other. The main objective is monitoring the condition of the Earth surface. This is possible that's to its wide observation band (290 km) and high review time (10 days at the equator with one satellite, and 5 days with 2 satellites in cloudless conditions, resulting in 2-3 days at mid-latitudes). The covertures limits are about the latitude 56° South and 84° North. In addition, it has a spatial resolution of 10 m, 20 m and 60 m (in the spectral range VNIR to SWIR) to identify constant special details with 1 ha as minimum unity of mapping.

The Sentinel-2 products available for users are a compilation of elementary granules of fixed size and with a single orbit. A granule, also called mosaic, is a 100×100 km^2 orthoimage in UTM/WGS84 projection. The UTM system (Universal Transverse Mercator) divides the Earth surface in 60 zones. Each UTM zone has a vertical width of 6° in longitude and a horizontal width of 8° latitude. Therefore, the granule is the minimum partition indivisible of one product (that contains all the spectral bands possible).

The analysis of the radiometric data quality is done by the specific Expert Support Laboratories (ESL). The quality requirements of the radiometry in the level 1 are:

- Absolute radiometric uncertainty: 3% (target), 5% (threshold)
- Relative radiometric uncertainty between bands: 3%
- Multi-temporal relative radiometric uncertainty: 1%
- Accuracy of linearity knowledge: 1%
- Channel-to-channel interference: < 0.5%
- Modulation Transfer Function (MTF): 0.15 to 0.3 (for 10 m bands) and < 0.45 (for 20 m and 60 m bands)

The objective of absolute radiometric precision is the 3%. To guarantee this high-quality radiometric performance, an integrated full-field and full-pupil diffuser is used.

Knowing the band equivalent wavelength is also very important because an error of 1 nm induces errors of several percent in the reflectance value, especially in the blue part and in the near-infrared region of the spectrum. The equivalent wavelength is known with an uncertainty of less than 1 nm. In the same way, an error in the absolute calibration

measurement affects in the precision of the physical value. For this sensor, the calibration precision between bands is 3% and the multi temporal calibration is about 1%. Furthermore, the non-linearity of the instrument response is more than 1% accurate and the channel-to-channel crosstalk is less than 0.5%.

The image quality depends on the MTF system, and has a value of about 0,15 and 0,3 in the Nyquist frequency for spectral bands with spectral resolution of 10 m and 20 m, and less of 0,45 for spectral bands with spatial resolution of 60 m.

The quality requirements of the geometric in the level 1 are:

- Absolute a priori geolocation uncertainty (before doing any processing): 2 km 3σ
- Absolute geolocation uncertainty: 20 m 2σ without GCP and 12.5 m 2σ with GCP
- Multi-temporal recording: 0.3 2σ pixels, including compensation for the effects of terrain height variation with an SRTM-class precision DEM and when image-to-image correlation is applied to data in the same spectral band
- Multispectral recording (for any two spectral bands): 0.3 pixels 3σ

All this performance requirements for the final data products are verified and validated by process and algorithms on board and on the ground corresponding to CAL-VAL activities that are responsibility of SENTINEL-2 Mission Performance Centre (MPC).

3.2.2.2 Radar satellite technology

There are several satellites put into orbit of for the detection of radar images (Figure 7) and their data can be accessed, although being most of them for private use. Currently, only the constellation Sentinel-1 offers its data for free. Therefore, its characteristics are to be described more detail in this section.

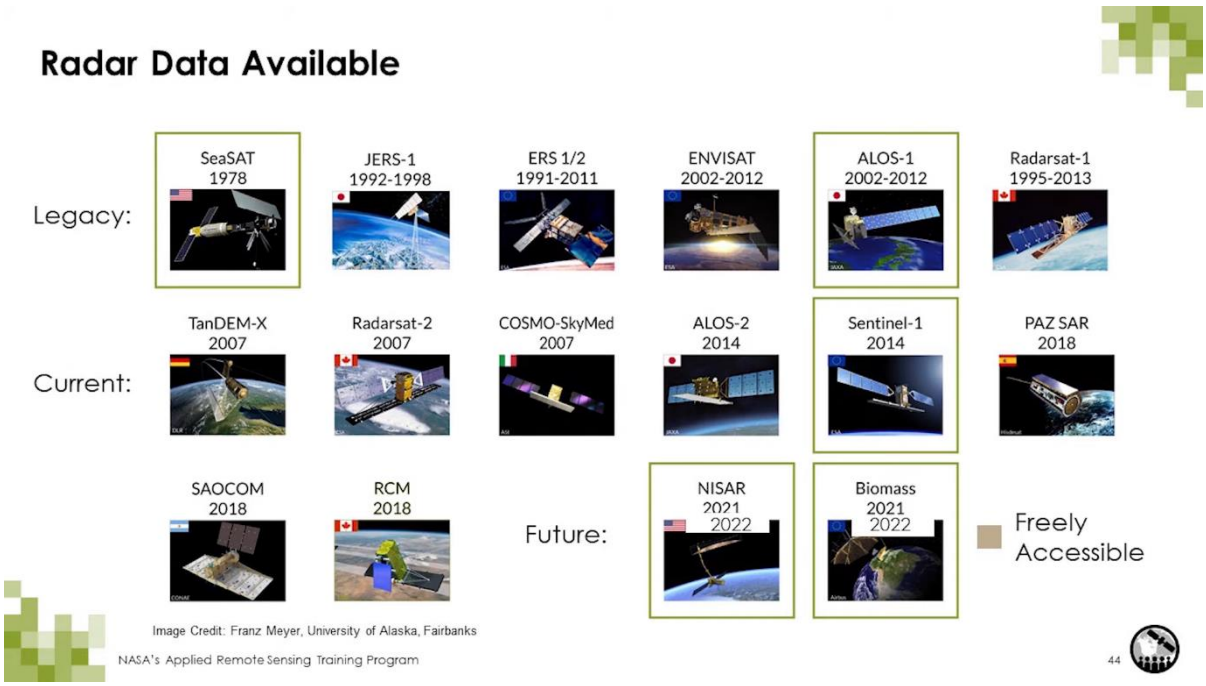

Figure 7: Main Radar platforms, detailing those that operate with free access (NASA, 2015)

In this way, focusing on the platforms that are currently operating, the following private satellites stand out:

- TanDEM-X: Its main objective is the Earth observation in all kinds of weather, including the vigilance and the management of the emergency. Specifically designed for the Digital Elevation Model (DEM) of 12×12 m in the Earth surface with vertical precision less than 2 m by interferometry with TerraSAR-X. In addition, it has contributed significantly to the temperature-humidity survey. Works in X-Band at 9.65 GHz, in spotlight mode have one Ground sampling distance (GSD) of 3 m.
- RadarSat-2: Its main function is the multi-purpose SAR observation, specially the ice. It works in C-Band at 5.405 GHz and with one resolution of 1×3 m in spotlight mode.
- COSMO-SkyMed: Its main objective is the vigilance and the management of the emergency. It works in X-Band at 9.6 GHz with a scan width of 10×10 km in spotlight mode and a geometric resolution of 1 m.
- ALOS-2: Its main objective is terrestrial observation, apart that has contributed substantially to the observation of the oceans. It works in the L band at 1.2 GHz and with a resolution of 3 m × 1 m in spotlight mode.
- SEOSAR / Paz: Its main objective is the vigilance and the management of the Earth, furthermore that has contributed substantially to the temperature-humidity survey and the detection of high precipitations. It works in X-Band at 9.6 GHz with a resolution in spotlight mode of 3 m × 3 m (Simple pol.) And 6 m × 6 m (Dual pol.).
- SAOCOM: Its main objective is the hydrological study and the Earth observation, apart, that has contributed substantially to the vigilance and the management of the emergency. It works in the L band at 1.275 GHz and with a resolution of 10 m × 5 m in spotlight mode.
- RCM: Its main function is the multi-purpose SAR observation, specially the ice, apart that has contributed to the vigilance and the management of the emergency. It works in C-Band at 5.405 GHz and with a resolution 3 m in Very high-resolution mode.

Nowadays, Sentinel-1 constellation is the only platform that provides free, systematic and open data. Its main mission is the multi-purpose, oceanic and land observation in high resolution and in all kinds of weather. Sentinel-1 is composed of a constellation of two satellites, Sentinel-1A and Sentinel-1B, that share the same orbital plane with an orbital phase difference of 180°. The mission provides an independent operative capacity for continuous radar mapping of the Earth with improved visit frequency, coverage, punctuality and reliability for operational services and applications requiring long time series.

Regarding its technical characteristics, it has:

- Synchronous near polar orbit with the sun and repeated 12-day cycle
- 4 operational modes:
  - Stripmap mode (SM): 80 km swath, 5 m×5 m resolution, single-look
  - Interferometric Wide Swath mode (IWS): 240 km swath, 5 m×20 m resolution, single-look
  - Extra-Wide Swath mode (EWS): 400 km swath, single-look

  - Interferometric Wide Swath mode (IWS): 240 km swath, 25 m×80 m resolution, 3-looks
  - Wave mode (WM): 20 km x 20 km, 20 m×5 m resolution, single-look
- Dual polarization for all VV + VH or HH + HV modes

Images for posterior analysis can downloaded through different free platforms. Level 1 Single Look Complex (SLC) products consist of SAR data, which are focus and georeferenced using orbital data and satellite attitude, and provided in zero Doppler tilted range geometry. The products include a single aspect in each dimension using the full bandwidth of the transmission signal and consist of complex samples that preserve phase information.

The products verification and the instrument processing (IPF), covers:

- Verification of the L0, L1 and L2 product format and main annotations
- Product family consistency, for example measurement consistency check for GRD HR, FR and MR
- Verification of the main processing algorithms:
  - Processing algorithm (Doppler estimation, focus, terrestrial range projection, deburring, stripe stitching)
  - Radiometric correction (antenna elevation patterns, TOPS scalloping, loss of range extension, etc.)
- IPF standardization:
  - Checking Image Dynamics and IPF Gain Settings
  - Radiometric sub-fringe fusion
  - Product performance evaluation:
    - Point target impulse response function analysis (spatial resolution and side lobes)
    - Ambiguity analysis (range and azimuth)
    - Radiometric resolution and equivalent number of loss measurements
    - Evaluation of the radar cross-section equivalent to noise
    - Geometric evaluation
- Burst timing evaluation

The L1 product calibration comprises:

- Absolute and relative radiometric calibration
- Polarimetric calibration
- Geometric calibration

The L2 geophysical validation comprises:

- Verification of geophysical variables against independent external measurements such as modal data, buoys or other source of EO data

4. Monitoring Scenarios in the Atlantic Area

4.1 Flooding-related events in Portugal / Sea level

4.1.1 Adverse events

Because cities are supported by impermeable soils, they have insufficient drainage capacity, which makes them more prone and vulnerable to urban flooding. This may be due to the increase in the intensity of the rains or to the rise in sea level. Historically, in Portugal, the natural threat that causes the greatest human damage is flooding. However, it is difficult to quantify material damage, since there is only information for very specific extreme events. One of the largest events occurred in the Lisbon Metropolitan Area (in which the following municipalities are included: Amadora, Cascais, Lisbon, Loures, Mafra, Odivelas, Oeiras, Sintra, Vila Franca de Xira, Alcochete, Almada, Barreiro, Moita, Montijo, Palmela, Seixal, Sesimbra and Setúbal) on February 18, 2008 (Leal et al., 2019). This Metropolitan Area is the one with the largest population in Portugal, so the risk of flooding or rising sea has a negative influence on the infrastructure network.

These extreme climatic events can cause numerous risks in the infrastructures such as the generalized interruption to the entire transmission network (Duy et al., 2019). Therefore, it is necessary to continuously monitor the state of the infrastructures in these areas due to their increasing vulnerability caused by climate change. To carry out effective monitoring, it is interesting to use a combination of techniques that can say how the current state of the infrastructures is presented. These techniques can be performed by total station, GPS, LiDAR, etc., but they generally tend to be related to a higher labour cost. That is why the InSAR technique is presented as a good monitoring alternative since it manages to analyse a very large study area with much lower costs and with good precision, in addition to the great availability of data from the past compared to those carried out with the other techniques (Strozzi et al., 2001; Suresh & Yarrakula, 2018).

4.1.2 Evaluation of scenarios

The objective is to demonstrate the use of the Mt-Insar technique for infrastructures monitoring. With this, a persistent Scatterer map will be obtained, in which each persistent Scatterer will give information about how much that point has moved over time. The map indicates the areas where displacements have occurred in the study structures, so that a better assessment can be made when making decisions in this regard.

The study area is the area from Lisbon to Cascais where there is both a road network (N6) and a railway network (Línea CASCAIS — CAIS DO SODRÉ) bordering the mouth of the river Tagus and the Atlantic Ocean, so this area is ideal for studying how events related to floods can affect infrastructures.

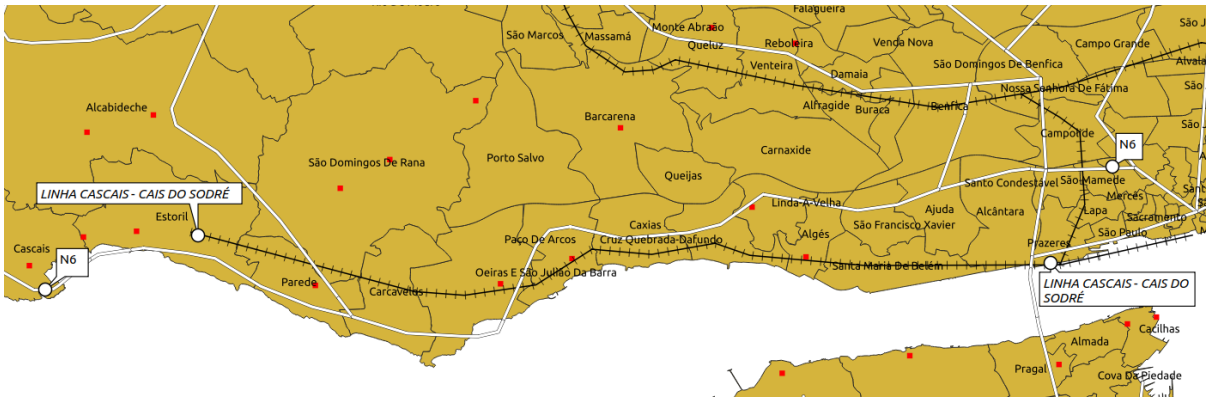

Figure 8: N6 Road and CASCAIS - CAIS DO SODRÉ train network Map (Forest-GIS, 2019)

4.2 Wildfires in Portugal

4.2.1 Adverse events

In the last decades, Europe registered a high number of fires and burnt area with different spatial and temporal trends as the result of human/driven fuel transformations and climate change (Vilar et al., 2016). Despite its smaller land area in comparison with other Mediterranean countries, Portugal is the European country with the highest total number of fires and the second largest total burnt area (Schmuck et al., 2015). The distribution of fire in Portugal presents a high spatial-temporal variability, being weather and climate variability the main drivers of the temporal distribution. The Mediterranean type of climate of mainland Portugal broadly controls the fire incidence's temporal and spatial variability (Parente et al., 2018). The occurrence of extreme weather (e.g., heat waves) and climate variability events (e.g., drought), which also tend to be more frequent and intense during the summer fire season, are main contributors to his sharp seasonal character of fire incidence in Portugal (Tonini et al., 2017).

The different subtype of climate in northern and southern Portugal also helps to understand why most of number of fires and burn area are located at north of the Tagus river. (Catry et al., 2007) studied the distribution of fire ignitions between 2001 and 2005 in Portugal and concluded that most of the fire ignitions were intentionally caused and concentrated in the most populated municipalities of the north and centre littoral areas. In the same way, (Parente et al., 2018) concluded that northern regions of the north and centre tend concentrate most of the fire incidence.

While forest fires became common place in the Portuguese continental territory, the events of 2017 are described as a new breed of fires, generating harsher consequences and damage. The wildfires of 2017 were one of the worst disasters to affect Portugal, with more than 275.845 hectares burnt from a yearly total of 424.000 hectares (Departamento de Gestão de Áreas Públicas e de Proteção Florestal (2017), 2017). In 2017, for the first wave of forest fires, most of the registered fatalities occurred when people attempted to flee from their homes by car, being caught by smoke and flames in main roads (Viegas, 2018).

4.2.2 Evaluation of scenarios

In 2018, the Southern region in Portugal was the most affected by forest fires. The literature retrieval will be considered for the definition of scenarios in the Portuguese pilot. Most of fires were registered in north Portugal. For this reason, the location selected was in Viana do Castelo district.

The focus of this pilot is to enhance the efficient management and mitigation of wildfire by developing fire risk maps around infrastructure networks as a short-term decision making.

- Generation of fuel and flammability models influencing in forest fire risk.
- Generate vegetation continuity covers and apply forest fire risk weather index based on the weather conditions.
- Short-term decision making over vegetation.
- Report on fire risks and establish the recommendations to road managers focusing on mitigation measure or actions.

The Pilot will take place in Portugal in the district of Viana do Castelo. It includes railway and road transportation modes (Figure 9). The Pilot was chosen due to the suffered forest fires in the last three years located in the vicinity of the railway and road network. In relation with the wildfires, the total area burnt in the years 2017, 2018 and 2019 were 425 Ha, 109 Ha and 690 Ha, respectively. Regarding the road section, it includes six sections which cover a total length of 25 km. Similarly, the railway area is subdivided in 3 sections of 16 km.

The information is organized as shown in the following scheme:

- Road: Sections 1, 2, 3, 4 and 7 are secondary routes with a length of 14 km, 5 km, 5.5 km, 900 m, and 6.8 km, respectively. Sections 5, 6 and 8 are primary routes with a length of 6.4 km, 2.7 km, and 1.2 km, respectively. All sections are in Valença district except for section 1 is in Paredes de Coura district.
- Railway: Section 1 (ID: 96485), section 2 (ID: 96497), section 3 (ID: 96319) and section 4 (ID:96488). All sections are in Valença district.

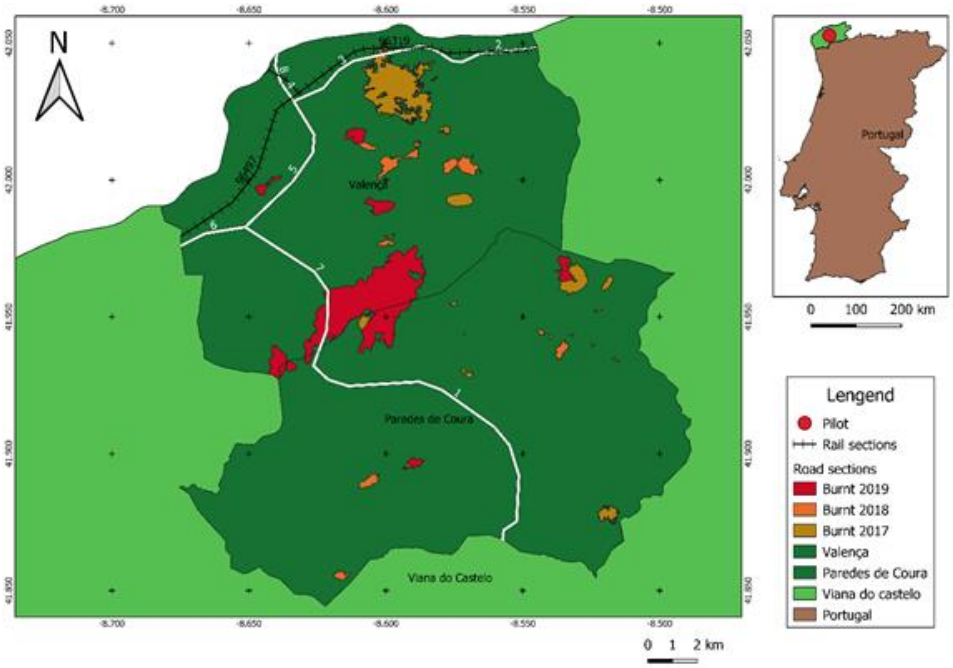

Figure 9: Pilot area location in Viana do Castelo, Portugal

5. Data Acquisition Protocols for the Monitoring of critical infrastructures in the Atlantic Area

This section presents a description of the data acquisition protocols to be followed depending on the remote sensing technology used of the ones exposed in Section 3. A first description is done for the terrestrial-based platforms, including not only protocols but also significant information needed for the performance of a survey. Then, a similar structure is followed for satellite technologies.

> ***Note:*** *Some information exposed in this section has been gathered from the datasheets of the products involved.*

5.1 Terrestrial-based platforms

This section describes the equipment necessary to perform a survey using terrestrial-based platforms. For the case of when it is necessary to obtain infrared data and/or RGB images, the equipment will be integrated with the mobile mapping system (MMS). Because of that, the protocols of these devices are explained together with the ones for the MMS.

5.1.1 Equipment

The mobile mapping system used in this project to gather LiDAR data is a Lynx mobile mapper (Lynx M1), from Optech. It controls four LiDAR sensors and two optional cameras, calibrated for the passive gathering of images. The operator controls the operations through a laptop connected to the command and control rack. The mobile mapper is usually combined with

different sensors so that other data can also be obtained. These sensors are placed in a platform on top of the vehicle, which has been developed by University of Vigo together with Optech. This set can be attached to a van, a wagon or a draisine, considering that the total weight is about 100 kg.

An essential parameter to be monitored is the position of the scanning system. This is performed through the combined use of:

- Global navigation satellite system (GNSS)
- Inertial measurement unit (IMU)
- Distance measurement indicators (DMI)

The positioning system available in this equipment is from APPLANIX (POS LV 520) and the GNSS receivers from TRIMBLE. With the coordinated use of these positioning devices it is possible to obtain the absolute location of the vehicle with respect to a global coordinate system (i.e. WGS84). Moreover, the LiDAR system stores the relative position of objects with respect to the MMS in a local coordinate system.

In addition, since the vehicle in which the system is installed is moving, it must follow a predefined trajectory while the scanner is registering data. This trajectory is also stored as a dense three dimensional point cloud in a global coordinate system. Each point represents position of the scanner when it is synchronised with the navigation system.

5.1.2 Hardware

5.1.2.1 Hardware installation

LiDAR. LiDAR sensors are installed on the frame of the MLS system, placed rear on the roof of the van, besides a box containing the INS and LiDAR rack in which the sensors and antennas are connected. The frame is covered with a protective shell, and both LiDAR sensor windows are protected with metallic covers that must be removed before each acquisition, checking for condensation on the windows and waiting to warm up if necessary. The laser emitted by the Lynx system is classified as “Class 1 Laser Product”, meaning it is sight-safe according to IEC 60825-1 rule.

Figure 10: Lynx laser scanner

Antennas. The GNSS antennas must be mounted with a minimum distance between them (at least 1.5 m, although the manufacturer recommends 2 m) to obtain a suitable accuracy.

Because of this requirement, the secondary antenna is placed in the front part of the roof of the van, as the primary antenna is fixed on top of the MLS shell.

Figure 11: Secondary GNSS antenna

DMI. The DMI must be installed on one of the non-directional wheels of the vehicle (thus, on the rear) with the provided bracket onto the bolts of the wheel's rim. The bracket has a rod attached to it, that must be slid through a plate on the side of the van, above the wheel, to maintain the DMI stabilized.

Figure 12: DMI mounted on the wheel

Control rack. The LiDAR rack, external RGB or thermographic cameras, DMI and other accessories are connected to the control rack, which is placed inside the vehicle and stores the information collected during the acquisition. A PC is connected to the rack, serving as an interface method and running the acquisition and control software.

Figure 13: Lynx control rack, installed in the floor inside the vehicle

360 camera. A camera can be installed to obtain 360° images. The camera is mounted on top of a pole on the centre of the vehicle's roof, at a certain height to avoid occlusions caused by the rest of the equipment.

Figure 14: Ladybug 360 camera

Cables. All cables must be firmly connected and, in the case of the devices mounted occasionally on the outside of the vehicle, disconnected after finishing.

5.1.2.2 Parameters setup

Lever arms between the INS (Inertial Navigation System), the reference frame centre, and all other sensors must be measured and introduced in the system for correctly referencing the collected data.

5.1.3 Survey protocols

This section describes the necessities to be considered when performing a survey with a mobile mapping system.

The most important requirement is to plan the survey before its performance. This will ensure the obtention of the best quality of data depending on the needs of each case study. The planification involves:

- Selection of equipment
- Preparation of the equipment

- Calibration of each device
- Selection of working parameters
- Definition of the trajectory

5.1.3.1 Meteorological conditions

Weather conditions must be the proper ones in order to obtain good results. Water drops and dust largely affect the measurements of the laser scanner, since it works in the visible light range. In addition, reflections may also be an issue when working with direct sunlight. For all these reasons, the better option would be a cloudy day without any fog or rain. This will help avoiding water drops or vapour affecting the measures or noise due to sun reflections.

Laser scanning surveys can be performed at any time of day or night, since LiDAR sensors are active. Depending on the data requirements, it would be necessary to do the gathering of data during the day to obtain RGB images, or due to navigation issues, among others. While the night surveys could also be useful for other aspects like reducing the traffic flow, reducing the interruptions of service, etc.

Lastly, although it does not depend that much on the meteorological conditions but on the time of the year, it is recommended to study the vegetation surrounding the survey area. The worst case for a survey is the existence of vegetation causing occlusions of relevant parts of the infrastructure (Filgueira et al., 2017; Belén Riveiro et al., 2015).

5.1.3.2 Accuracy improvement

The accuracy of the gathered data depends on several factors:

- Geometrical characteristics of the scenario
- Equipment
- Speed of the vehicle

The calibration of the equipment must be done before the data gathering and ensuring some conditions. A minimum of 200-300 m outdoors is necessary for calibrating the sensors before entering a tunnel or a railway environment. The accuracy of the trajectory can also be improved by stopping the moving platform for at least 10 minutes at the beginning and ending of the itinerary, so that the GNSS can get a good coverage. Finally, the vehicle carrying the platform of the sensors must be moving at a constant speed, with a maximum of 30-40 km/h.

5.2 Satellite resources

5.2.1 Existing EU programs

To get a global vision of the Earth health condition through the Global Earth Observation Systems of Systems (GEOSS) it is intended to facilitate and standardize the access to satellite data of the different information sources. For that purpose, the European Union, based in a satellite constellation through the European Space Agency and under the Sentinel program which includes observations by radar images in wide spectrum for the monitoring of continents, oceans and the atmosphere, has its own provider of spatial data (Copernicus) being this the largest provider in the world, currently producing 12 terabytes per day.

The majority of data and information of the Copernicus Space infrastructure and the Copernicus service are available and accessible for any citizen and any organization all over the world, openly and free of charge. Copernicus data and information services can be accessed through DIAS or through Conventional Data Access Hubs.

DIAS (Data and Information Access Services):

The European Commission has funded the launching of five cloud-based platforms (open source and/or pay-per-use) that provide centralized access to Copernicus data and information, as well as to the processing tools. Thanks to the existence of a single access point for the all Copernicus data and information, DIAS make possible that the users develop and lodge their own applications in the cloud, avoiding the need of downloading large files from various access spots for local processing. The existence of several DIAS is presented as a way to offer diversity to users and to promote competition among them with the confidence that this will result in a better offer.

- ONDA: It is a platform whose users can save data and create applications in the Cloud.
- CREODIAS: It is a platform in the Cloud that adapts to the processing of big amounts of Earth Observation data, including an EO data storage cluster and a dedicated cloud infrastructure for platform users. The EO repository contains data from the Sentinel-1, 2 and 3, Landsat-5, 7, 8, Envisat and many Copernicus services data. The access to the satellite images and its download is free, charging for services such as analysis tools, storage, etc.
- Mundi Web Services: Offers to the users and companies unlimited, free and complete access to the Copernicus satellite data in real time and permits to combine them with their own data and tools to create new products and services that integrate accurate and real-time information from the different satellites. The access to the offered service is made by two types of account: standard and premium.
- Sobloo: It has been designed to accommodate all user profiles with different entry points and capabilities. It is an open geospatial community for the people that needs data and associate service, and for developers that need a dedicated environment to build applications.
- WEkEO: It is a platform in the Cloud which provides environmental data, virtual processing environments and support for qualified users.

Conventional Data Access Hubs:

The European Space Agency (ESA) manages two data access points from the Copernicus satellite:

- Copernicus Open Access Hub: The portal provides access to Sentinel data through two types of interfaces: an interactive graphical interface and another application programming interface (API).
- Copernicus Space Component Data Access (CSCDA): The portal provides access to the Copernicus collaborative terrain segment. Anyone can access the data, but downloading of images is restricted to public authorities, European projects and Copernicus services.

EUMETSAT manages two access points to the Copernicus satellite data:

- EUMETCast: The portal provides access to environmental data in any format.
- Copernicus Online Data Access (CODA): Provides free and open access to Sentinel-3 products through a continuous 12-month archive with access to Level 1 and Level 2 marine data in different latency modes.

5.2.2 Protocols to access, download and pre-process data

The Copernicus Open Access Hub is the recommended access point for downloading Copernicus data since it is the easiest to use.

To access the data, any user must previously register on the platform through a simple self-registration form that implies the recognition of the general terms and conditions for the use and distribution of Copernicus Sentinel data (Figure 15 and Figure 16).

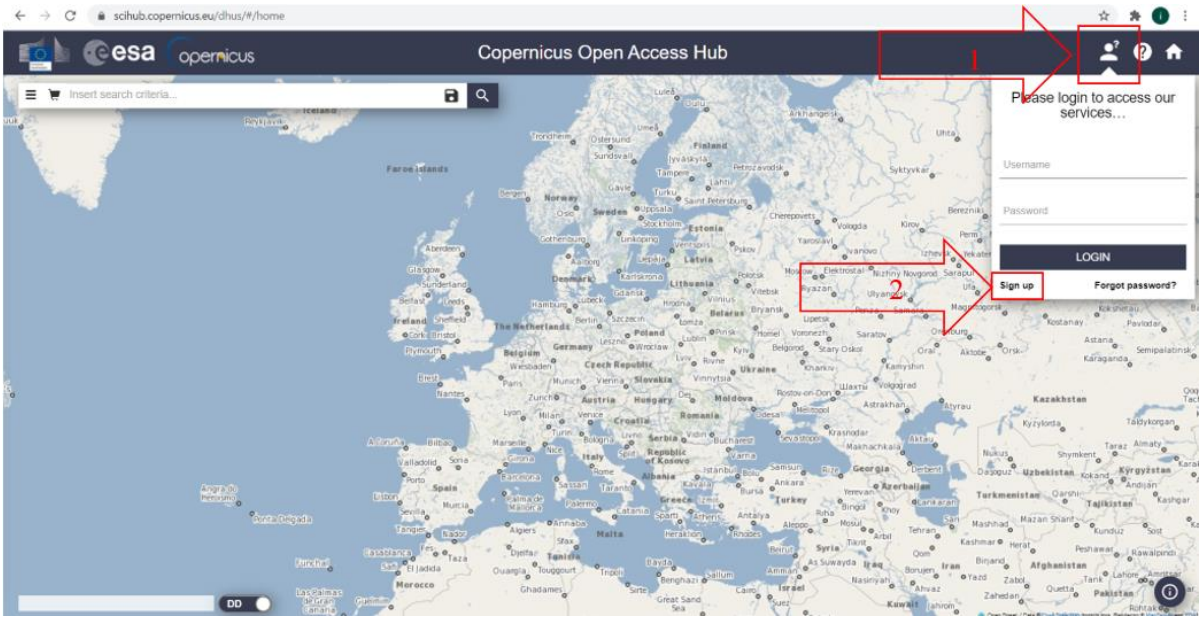

Figure 15: Registry access

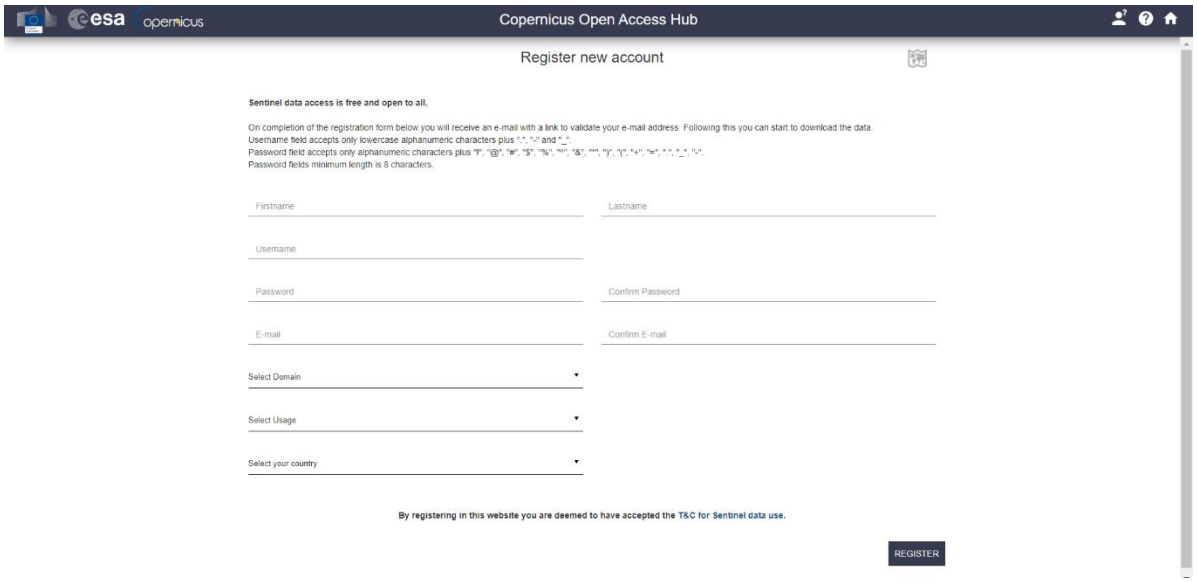

Figure 16: Registration Form

Once registered, the user can download the images (with a maximum of two images simultaneously), selecting the Sentinel product that are interesting to be analysed. This download could be made by the interactive graphic user interface or by the API, via a scripted interface as this ensures better download performance. Here, a guide is given through the interactive graphic user interface, since it is easier to use for the average user and it does not require previous programming knowledge.

The study area of interest must be selected (in orange box) (step 3 and 4, Figure 17).

Once the study area has been selected, the data to be analysed must be filtered (step 5, Figure 18).

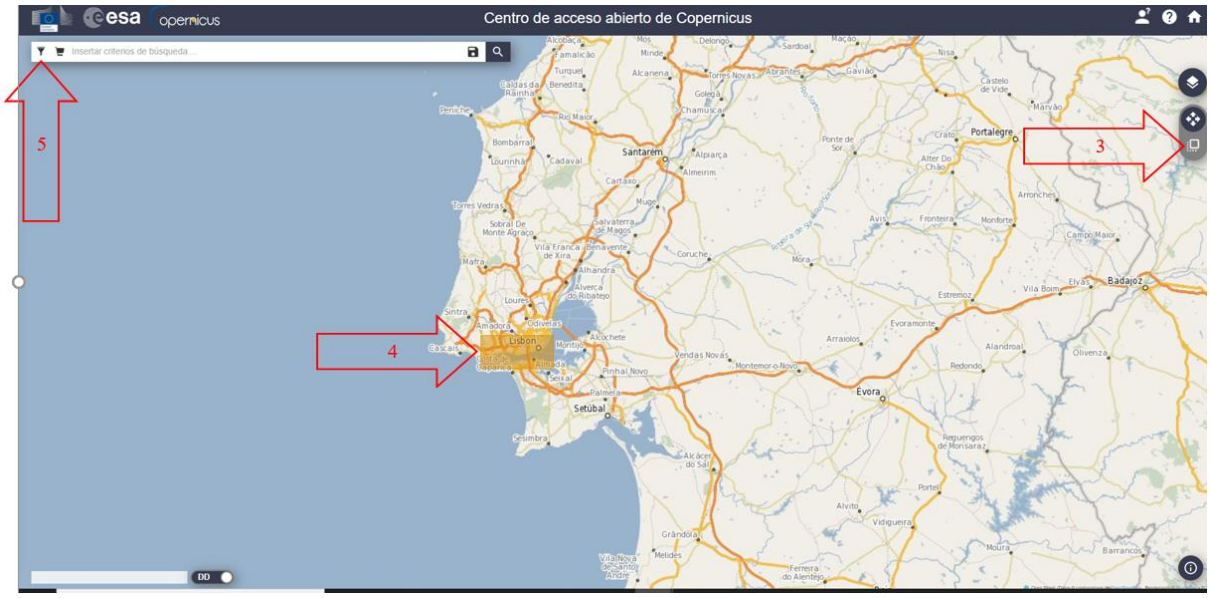

Figure 17: Selection of region of interest (ROI)

To do this, the user must specify in the advanced search the detection period in which the analysis is located and if ascending or descending capture is required. In addition, the user must specify in the Sentinel-1 boxes, which of the two platforms must be used. Finally, it is necessary to check the SLC options in the product type and in the VV polarization box. The rest of the boxes can remain unfilled.

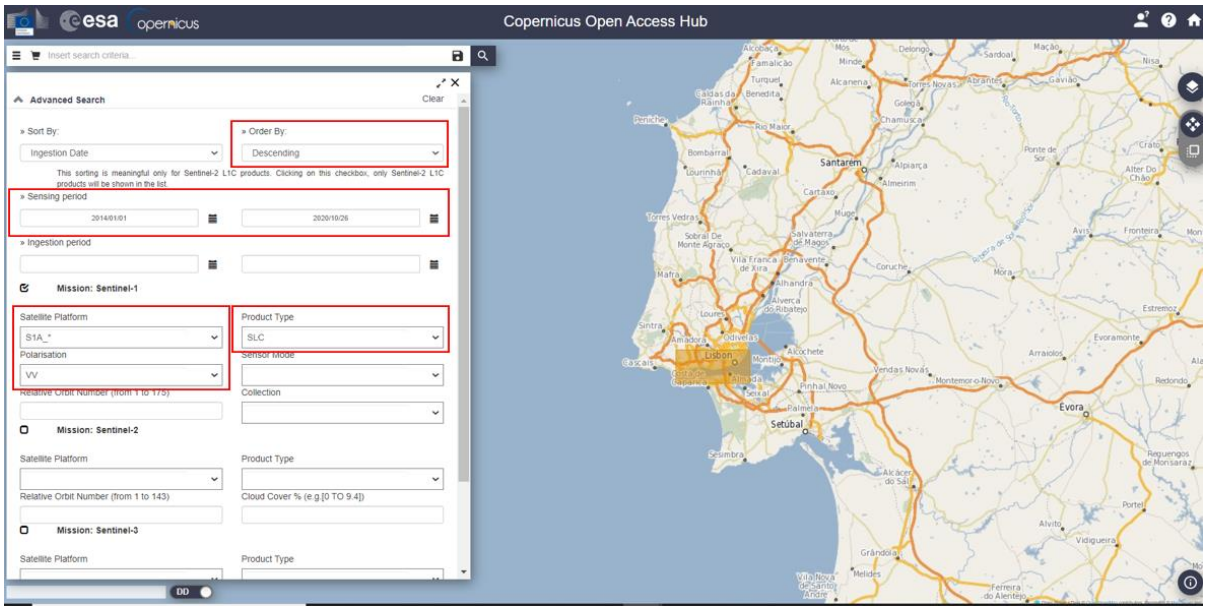

Figure 18: Data filtering

Once this is done, the list of all the images of the study area available is obtained (Figure 19), in order to select the appropriate one and download it (step 6, Figure 20-Figure 22). The downloading process can take several minutes, due to the weight of the images and the oldest images are already archived offline. Therefore, they are not available for direct download. So, if the user wants to download them, this must be requested so that within a few hours, the possibility of downloading them is activated.

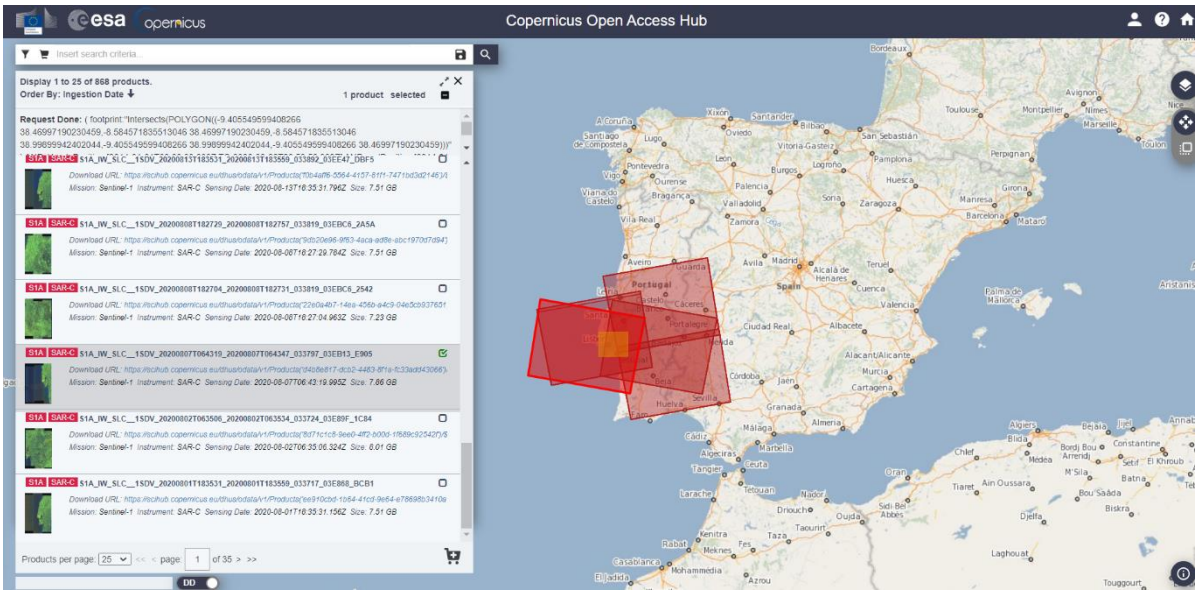

Figure 19: Available products and selection of the product to be analysed

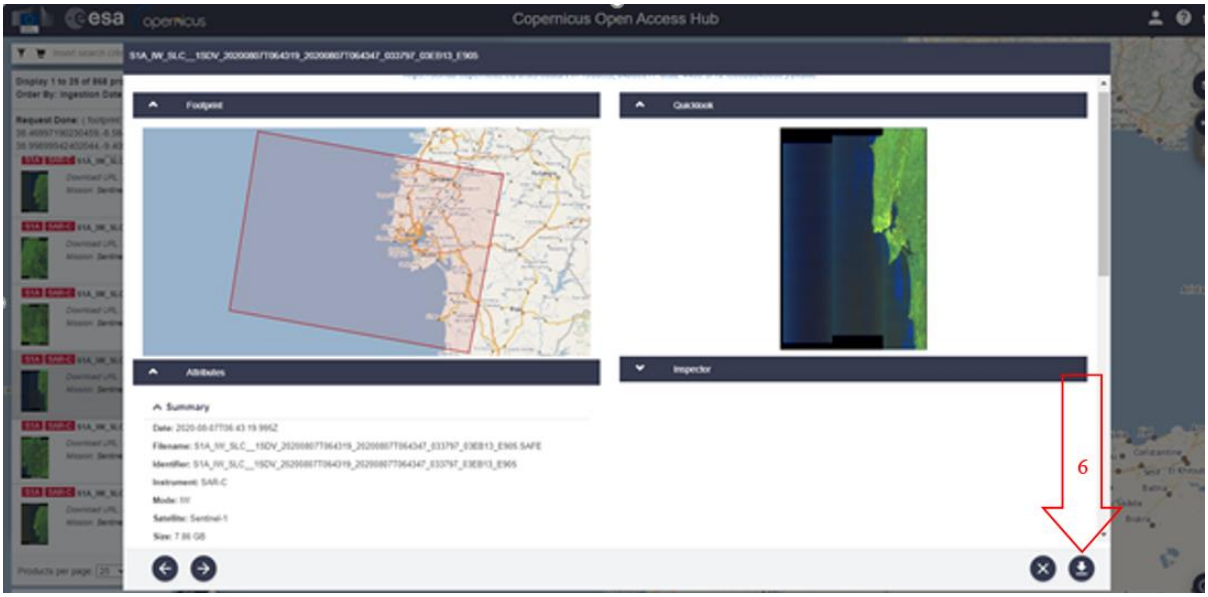

Figure 20: Technical description of the parameters of the selected products and download button

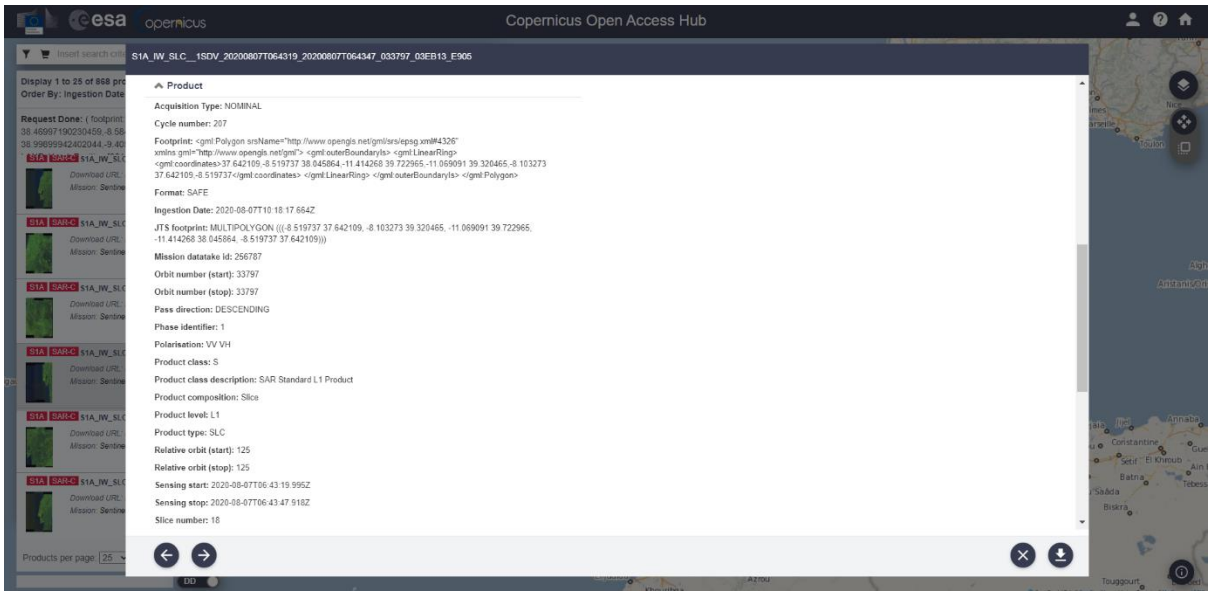

Figure 21: Technical description of the parameters of the selected products

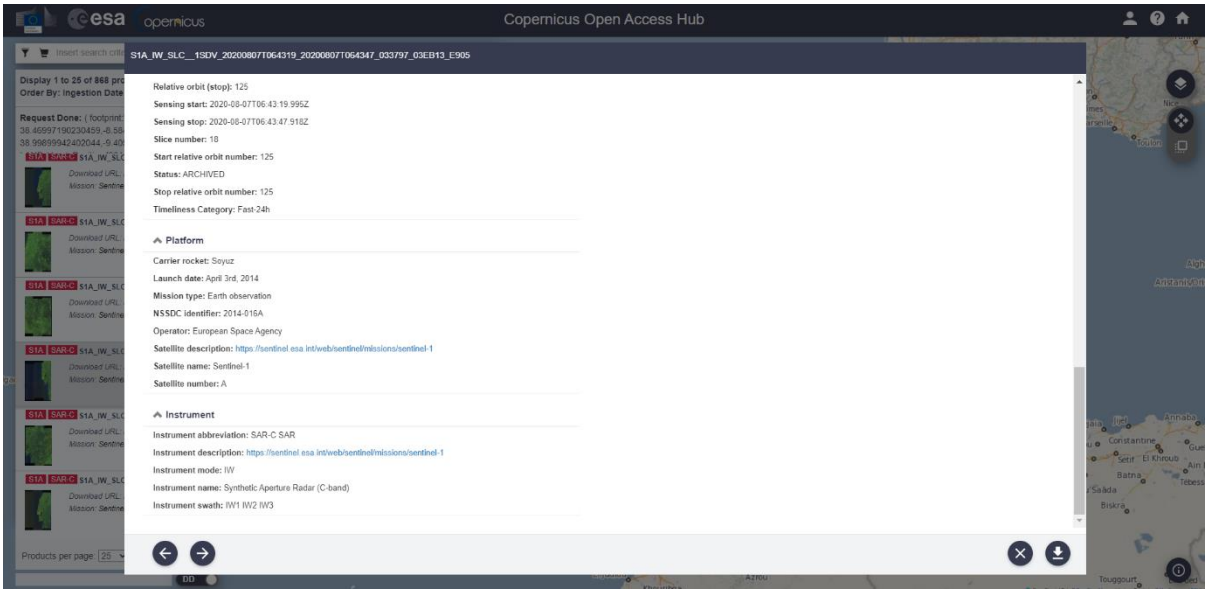

Figure 22: Technical description of the parameters of the selected products

Finally, two free access programs are recommended for data processing. For both radar and optical images, the use of SNAP is recommended as it is supported by the European Space Agency since it gives an easy intuitive graphic interface for the prosecution of data. For radar images the free program StaMPS/MTI can also be used. Designed in the original version by the Stanford University, this program is especially focused on the detection of displacements in a time series by the Permanent Scatterers of InSAR technique through programming and commands in a MATLAB environment.

Acknowledgements

This report was carried out in the framework of the Strengthening the Territory's Resilience to Risks of Natural, Climate and Human Origin (SIRMA) project, which is co-financed by the European Regional Development Fund (ERDF) through INTERREG Atlantic Area Programme with application code: EAPA_826/2018.

The sole responsibility for the content of this publication lies with the authors. It does not necessarily reflect the opinion of the European Union. Neither the INTERREG Europe programme authorities are responsible for any use that may be made of the information contained therein.

References

Al-Bayari, O. (2019). Mobile mapping systems in civil engineering projects (case studies). *Applied Geomatics*, *11*(1), 1–13. https://doi.org/10.1007/s12518-018-0222-6

Arastounia, M. (2012). Automatic Classification of LiDAR Point Clouds in A Railway Environment. *University of Twente, Netherlands*.

Arastounia, M. (2015). Automated Recognition of Railroad Infrastructure in Rural Areas from LIDAR Data. *Remote Sensing*, *7*(11), 14916–14938. https://doi.org/10.3390/rs71114916

Arastounia, M. (2017). An Enhanced Algorithm for Concurrent Recognition of Rail Tracks and Power Cables from Terrestrial and Airborne LiDAR Point Clouds. *Infrastructures*, *2*(2), 8. https://doi.org/10.3390/infrastructures2020008

Arastounia, M., & Elberink, S. O. (2016). *Application of Template Matching for Improving Classification of Urban Railroad Point Clouds*. https://doi.org/10.3390/s16122112

Arias, P., Riveiro, B., Soilán, M., Díaz-Vilariño, L., & Martínez-Sánchez, J. (2015). Simple Approaches To Improve the Automatic Inventory of Zebra Crossing From Mls Data. *ISPRS - International Archives of the Photogrammetry, Remote Sensing and Spatial Information Sciences*, *XL-3/W3*, 103–108. https://doi.org/10.5194/isprsarchives-XL-3-W3-103-2015

Ariyachandra, M. F., & Brilakis, I. (2020a). Detection of Railway Masts in Airborne LiDAR Data. *Journal of Construction Engineering and Management*, *146*(9), 04020105. https://doi.org/10.1061/(ASCE)CO.1943-7862.0001894

Ariyachandra, M. F., & Brilakis, I. (2020b, October 14). Digital Twinning of Railway Overhead Line Equipment from Airborne LiDAR Data. *Proceedings of the 37th International Symposium on Automation and Robotics in Construction (ISARC)*. https://doi.org/10.22260/isarc2020/0174

Artagan, S. S., Bianchini Ciampoli, L., D'Amico, F., Calvi, A., & Tosti, F. (2020). Non-destructive Assessment and Health Monitoring of Railway Infrastructures. In *Surveys in Geophysics* (Vol. 41, Issue 3, pp. 447–483). Springer. https://doi.org/10.1007/s10712-019-09544-w

Bakon, M., Perissin, D., Lazecky, M., & Papco, J. (2014). Infrastructure Non-linear Deformation Monitoring Via Satellite Radar Interferometry. *Procedia Technology*, *16*, 294–300. https://doi.org/10.1016/j.protcy.2014.10.095

Beger, R., Gedrange, C., Hecht, R., & Neubert, M. (2011). Data fusion of extremely high resolution aerial imagery and LiDAR data for automated railroad centre line reconstruction. *ISPRS Journal of Photogrammetry and Remote Sensing*, *66*(6), S40–S51. https://doi.org/10.1016/j.isprsjprs.2011.09.012

Cabo, C., Ordoñez, C., García-Cortés, S., & Martínez, J. (2014). An algorithm for automatic detection of pole-like street furniture objects from Mobile Laser Scanner point clouds. *ISPRS Journal of Photogrammetry and Remote Sensing*, *87*, 47–56. https://doi.org/10.1016/j.isprsjprs.2013.10.008

Catry, F. X., Damasceno, P., Silva, J. S., Galante, M., & Moreira, F. (2007). Spatial distribution patterns of wildfire ignitions in Portugal. *Modelação Espacial Do Risco de Ignição Em Portugal Continental*, 8.

Chamoso, P., González-Briones, A., De La Prieta, F., & Corchado, J. M. (2018). Computer vision system for fire detection and report using UAVs. *RSFF*, 40–49.

Chang, L., Dollevoet, R. P. B. J., & Hanssen, R. F. (2017). Nationwide Railway Monitoring Using Satellite SAR Interferometry. *IEEE Journal of Selected Topics in Applied Earth Observations and Remote Sensing*, *10*(2), 596–604. https://doi.org/10.1109/JSTARS.2016.2584783

Che, E., Jung, J., & Olsen, M. (2019). Object Recognition, Segmentation, and Classification of Mobile Laser Scanning Point Clouds: A State of the Art Review. *Sensors*, *19*(4), 810. https://doi.org/10.3390/s19040810

Chen, P., Wang, P., Lauer, M., Tang, X., & Wang, J. (2017). A rail wear measurement method based on structured light scanning. In A. V. Bernstein, A. Olaru, & J. Zhou (Eds.), *2016 International Conference on Robotics and Machine Vision* (Vol. 10253, p. 102530J). https://doi.org/10.1117/12.2266469

Chen, X., & Li, J. (2016). A feasibility study on use of generic mobile laser scanning system for detecting asphalt pavement cracks. *International Archives of the Photogrammetry, Remote Sensing and Spatial Information Sciences - ISPRS Archives*, *2016-Janua*(July), 545–549. https://doi.org/10.5194/isprsarchives-XLI-B1-545-2016

Cheng, Y. J., Qiu, W. G., & Duan, D. Y. (2019). Automatic creation of as-is building information model from single-track railway tunnel point clouds. *Automation in Construction*, *106*, 102911. https://doi.org/10.1016/j.autcon.2019.102911

Conedera, M., Tonini, M., Oleggini, L., Orozco, C. V., Leuenberger, M., & Pezzatti, G. B. (2015). Geospatial approach for defining the Wildland-Urban Interface in the Alpine environment. *Computers, Environment and Urban Systems*, *52*, 10–20.

Corongiu, M., Masiero, A., & Tucci, G. (2020). Classification of railway assets in mobile mapping point clouds. *International Archives of the Photogrammetry, Remote Sensing and Spatial Information Sciences - ISPRS Archives*, *43*(B1), 219–225. https://doi.org/10.5194/isprs-archives-XLIII-B1-2020-219-2020

Cserép, M., & Mayer, F. (2020). *Powerline tracking and extraction from dense LiDAR point clouds*. Eötvös Loránd University.

Delgado Blasco, J., Foumelis, M., Stewart, C., & Hooper, A. (2019). Measuring Urban Subsidence in the Rome Metropolitan Area (Italy) with Sentinel-1 SNAP-StaMPS Persistent Scatterer Interferometry. *Remote Sensing*, *11*(2), 129. https://doi.org/10.3390/rs11020129

Departamento de Gestão de Áreas Públicas e de Proteção Florestal (2017). (2017). *"Relatório provisório de incêndios florestais: Informação estatística sobre áreas ardidas e ocorrências", 1 de Janeiro a 31 de Outubro de 2017 (No. RIF10/2017).*

Ding, L., Zhang, H., Li, B., Xiao, J., Lu, S., & Klette, R. (2019). Improved road marking detection

and recognition. *Proceedings - 2018 15th International Symposium on Pervasive Systems, Algorithms and Networks, I-SPAN 2018*. https://doi.org/10.1109/I-SPAN.2018.00047

Duy, P. N., Chapman, L., & Tight, M. (2019). Resilient transport systems to reduce urban vulnerability to floods in emerging-coastal cities: A case study of Ho Chi Minh City, Vietnam. *Travel Behaviour and Society*, *15*, 28–43. https://doi.org/10.1016/j.tbs.2018.11.001

El Gamal, A., & Eltoukhy, H. (2005). CMOS image sensors. *IEEE Circuits and Devices Magazine*, *21*(3), 6–20. https://doi.org/10.1109/MCD.2005.1438751

Elberink, S., & Khoshelham, K. (2015). Automatic Extraction of Railroad Centerlines from Mobile Laser Scanning Data. *Remote Sensing*, *7*(5), 5565–5583. https://doi.org/10.3390/rs70505565

European Space Agency. (2014). *ESA - Sentinel-1*. http://www.esa.int/Applications/Observing_the_Earth/Copernicus/Sentinel-1

European Space Agency. (2015). *ESA - Sentinel-2*. http://www.esa.int/Applications/Observing_the_Earth/Copernicus/Sentinel-2

Falamarzi, A., Moridpour, S., & Nazem, M. (2019). A Review on Existing Sensors and Devices for Inspecting Railway Infrastructure. *Jurnal Kejuruteraan*, *31*(1), 1–10. https://doi.org/10.17576/jkukm-2019-31(1)-01

Filgueira, A., González-Jorge, H., Lagüela, S., Díaz-Vilariño, L., & Arias, P. (2017). Quantifying the influence of rain in LiDAR performance. *Measurement*, *95*, 143–148. https://doi.org/10.1016/j.measurement.2016.10.009

Fischler, M. A., & Bolles, R. C. (1981). Random sample consensus: a paradigm for model fitting with applications to image analysis and automated cartography. *Communications of the ACM*. https://doi.org/10.1145/358669.358692

Forest-GIS. (2019). *PORTUGAL: Shapefiles gerais de todo o país*. Http://Forest-Gis.Com/2012/01/Portugal-Shapefiles-Gerais-Do-Pais.Html/. http://forest-gis.com/2012/01/portugal-shapefiles-gerais-do-pais.html/

Freden, S. C., Mercanti, E. P., & Becker, M. A. (1974). *Third Earth Resources Technology Satellite-1 Symposium: The Proceedings of a Symposium Held by Goddard Space Flight Center at Washington, DC on December 10-14, 1973: Prepared at Goddard Space Flight Center* (Vol. 351). Scientific and Technical Information Office, National Aeronautics and Space ….

Fu, L., Chang, S., & Liu, C. (2018). Automatic measuring method of catenary geometric parameters based on laser scanning and imaging. In J. Zhu, K. Xu, L. Dong, H.-Y. Tam, & H. Xiao (Eds.), *2017 International Conference on Optical Instruments and Technology: Optoelectronic Measurement Technology and Systems* (p. 75). SPIE. https://doi.org/10.1117/12.2295340

Ganteaume, A., Camia, A., Jappiot, M., San-Miguel-Ayanz, J., Long-Fournel, M., & Lampin, C. (2013). A review of the main driving factors of forest fire ignition over Europe. *Environmental Management*, *51*(3), 651–662.

García, M., Riaño, D., Chuvieco, E., Salas, J., & Danson, F. M. (2011). Multispectral and LiDAR data fusion for fuel type mapping using Support Vector Machine and decision rules. *Remote Sensing of Environment*, *115*(6), 1369–1379.

García, M., Saatchi, S., Ustin, S., & Balzter, H. (2018). Modelling forest canopy height by integrating airborne LiDAR samples with satellite Radar and multispectral imagery. *International Journal of Applied Earth Observation and Geoinformation*, *66*, 159–173.

Gordon, C. E., Price, O. F., & Tasker, E. M. (2017). Mapping and exploring variation in post-fire vegetation recovery following mixed severity wildfire using airborne LiDAR. *Ecological Applications : A Publication of the Ecological Society of America*, *27*(5), 1618–1632. https://doi.org/10.1002/eap.1555

Guan, H., Li, J., Yu, Y., Chapman, M., Wang, H., Wang, C., & Zhai, R. (2015). Iterative tensor voting for pavement crack extraction using mobile laser scanning data. *IEEE Transactions on Geoscience and Remote Sensing*, *53*(3), 1527–1537. https://doi.org/10.1109/TGRS.2014.2344714

Guan, H., Yu, Y., Ji, Z., Li, J., & Zhang, Q. (2015). Deep learning-based tree classification using mobile LiDAR data. *Remote Sensing Letters*. https://doi.org/10.1080/2150704X.2015.1088668

Gucinski, H., Furniss, M. J., Ziemer, R. R., & Brookes, M. H. (2001). Forest roads: A synthesis of scientific information. *General Technical Reports of the US Department of Agriculture, Forest Service*, *509*, 1–103.

Gudigar, A., Chokkadi, S., Raghavendra, U., & Acharya, U. R. (2019). An efficient traffic sign recognition based on graph embedding features. *Neural Computing and Applications*. https://doi.org/10.1007/s00521-017-3063-z

Guo, B., Li, Q., Huang, X., & Wang, C. (2016). An Improved Method for Power-Line Reconstruction from Point Cloud Data. *Remote Sensing*, *8*(1), 36. https://doi.org/10.3390/rs8010036

Guo, F., Su, Z., Wang, G., Sun, L., Lin, F., & Liu, A. (2016). Wildfire ignition in the forests of southeast China: Identifying drivers and spatial distribution to predict wildfire likelihood. *Applied Geography*, *66*, 12–21.

Hackel, T., Stein, D., Maindorfer, I., Lauer, M., & Reiterer, A. (2015). Track detection in 3D laser scanning data of railway infrastructure. *2015 IEEE International Instrumentation and Measurement Technology Conference (I2MTC) Proceedings*, *2015-July*, 693–698. https://doi.org/10.1109/I2MTC.2015.7151352

Hamraz, H., Contreras, M. A., & Zhang, J. (2017). Vertical stratification of forest canopy for segmentation of understory trees within small-footprint airborne LiDAR point clouds. *ISPRS Journal of Photogrammetry and Remote Sensing*, *130*, 385–392.

Hong, H., Tsangaratos, P., Ilia, I., Liu, J., Zhu, A.-X., & Xu, C. (2018). Applying genetic algorithms to set the optimal combination of forest fire related variables and model forest fire susceptibility based on data mining models. The case of Dayu County, China. *Science of the Total Environment*, *630*, 1044–1056.

Hulin, B., & Schussler, S. (2005). Measuring vegetation along railway tracks. *Proceedings. 2005 IEEE Intelligent Transportation Systems, 2005.*, 561–565.

Jain, A., Mishra, A., Shukla, A., & Tiwari, R. (2019). A Novel Genetically Optimized Convolutional Neural Network for Traffic Sign Recognition: A New Benchmark on Belgium and Chinese Traffic Sign Datasets. *Neural Processing Letters*. https://doi.org/10.1007/s11063-019-09991-x

Jeon, W. G., & Choi, B. G. (2013). A Study on the Automatic Detection of Railroad Power Lines Using LiDAR Data and RANSAC Algorithm. *Journal of the Korean Society of Surveying, Geodesy, Photogrammetry and Cartography*, *31*(4), 331–339. https://doi.org/10.7848/ksgpc.2013.31.4.331

Jia, H., Wei, Z., He, X., Lv, Y., He, D., & Li, M. (2018). Biologically Visual Perceptual Model and Discriminative Model for Road Markings Detection and Recognition. *Mathematical Problems in Engineering*. https://doi.org/10.1155/2018/6062081

Jolliffe, I. T. (1986). *Principal Component Analysis and Factor Analysis* (pp. 115–128). Springer, New York, NY. https://doi.org/10.1007/978-1-4757-1904-8_7

Jung, J., Chen, L., Sohn, G., Luo, C., & Won, J.-U. (2016). Multi-Range Conditional Random Field for Classifying Railway Electrification System Objects Using Mobile Laser Scanning Data. *Remote Sensing*, *8*(12), 1008. https://doi.org/10.3390/rs8121008

Kane, V. R., North, M. P., Lutz, J. A., Churchill, D. J., Roberts, S. L., Smith, D. F., McGaughey, R. J., Kane, J. T., & Brooks, M. L. (2014). Assessing fire effects on forest spatial structure using a fusion of Landsat and airborne LiDAR data in Yosemite National Park. *Remote Sensing of Environment*, *151*, 89–101.

Karagiannis, G., Olsen, S., & Pedersen, K. (2020). Deep Learning for Detection of Railway Signs and Signals. *Advances in Intelligent Systems and Computing*, *943*, 1–15. https://doi.org/10.1007/978-3-030-17795-9_1

Kim, B., & Cho, S. (2018). *Automated Vision-Based Detection of Cracks on Concrete Surfaces Using a Deep Learning Technique*. *2013*. https://doi.org/10.3390/s18103452

Kükenbrink, D., Schneider, F. D., Leiterer, R., Schaepman, M. E., & Morsdorf, F. (2017). Quantification of hidden canopy volume of airborne laser scanning data using a voxel traversal algorithm. *Remote Sensing of Environment*, *194*, 424–436.

Kumar, P., McElhinney, C. P., Lewis, P., & McCarthy, T. (2013). An automated algorithm for extracting road edges from terrestrial mobile LiDAR data. *ISPRS Journal of Photogrammetry and Remote Sensing*, *85*(2013), 44–55. https://doi.org/10.1016/j.isprsjprs.2013.08.003

Leal, M., Boavida-Portugal, I., Fragoso, M., & Ramos, C. (2019). How much does an extreme rainfall event cost? Material damage and relationships between insurance, rainfall, land cover and urban flooding. *Hydrological Sciences Journal*, *64*(6), 673–689. https://doi.org/10.1080/02626667.2019.1595625

Leslar, M., Perry, G., & McNease, K. (2010). Using mobile lidar to survey a railway line for asset inventory. *American Society for Photogrammetry and Remote Sensing Annual Conference*

2010: Opportunities for Emerging Geospatial Technologies, 526–533.

Liang, X., Wang, Y., Pyörälä, J., Lehtomäki, M., Yu, X., Kaartinen, H., Kukko, A., Honkavaara, E., Issaoui, A. E. I., Nevalainen, O., Vaaja, M., Virtanen, J.-P., Katoh, M., & Deng, S. (2019). Forest in situ observations using unmanned aerial vehicle as an alternative of terrestrial measurements. *Forest Ecosystems*, *6*(1), 20. https://doi.org/10.1186/s40663-019-0173-3

Lou, Y., Zhang, T., Tang, J., Song, W., Zhang, Y., & Chen, L. (2018). A Fast Algorithm for Rail Extraction Using Mobile Laser Scanning Data. *Remote Sensing*, *10*(12), 1998. https://doi.org/10.3390/rs10121998

Matson, K. C., Day, P., Hinnant, L., Fernandez, A. O., & Back, E. (2018). *Vegetation detection and alert system for a railway vehicle*. Google Patents.

Mikrut, S., Kohut, P., Pyka, K., Tokarczyk, R., Barszcz, T., & Uhl, T. (2016). Mobile Laser Scanning Systems for Measuring the Clearance Gauge of Railways: State of Play, Testing and Outlook. *Sensors*, *16*(5), 683. https://doi.org/10.3390/s16050683

Minbashi, N., Bagheri, M., Golroo, A., Arasteh Khouy, I., & Ahmadi, A. (2016). Turnout Degradation Modelling Using New Inspection Technologies: A Literature Review. *Lecture Notes in Mechanical Engineering*. https://doi.org/10.1007/978-3-319-23597-4_5

Molina, J. R., Lora, A., Prades, C., & y Silva, F. R. (2019). Roadside vegetation planning and conservation: New approach to prevent and mitigate wildfires based on fire ignition potential. *Forest Ecology and Management*, *444*, 163–173.

NASA. (2015). *NASA Applied Remote Sensing Training*. https://appliedsciences.nasa.gov/what-we-do/capacity-building/arset

Navarro, G., Caballero, I., Silva, G., Parra, P.-C., Vázquez, Á., & Caldeira, R. (2017). Evaluation of forest fire on Madeira Island using Sentinel-2A MSI imagery. *International Journal of Applied Earth Observation and Geoinformation*, *58*, 97–106.

Niina, Y., Honma, R., Honma, Y., Kondo, K., Tsuji, K., Hiramatsu, T., & Oketani, E. (2018). Automatic rail extraction and clearance check with a point cloud captured by MLS in a Railway. *International Archives of the Photogrammetry, Remote Sensing and Spatial Information Sciences - ISPRS Archives*, *42*(2), 767–771. https://doi.org/10.5194/isprs-archives-XLII-2-767-2018

Nuttens, T., Breuck, V. D. E., Cattoor, R., Decock, K., & Hemeryck, I. (2018). Using bim models for the design of large rail infrastructure projects: Key factors for a successful implementation. *International Journal of Sustainable Development and Planning*, *13*(1), 73–83. https://doi.org/10.2495/SDP-V13-N1-73-83

Nyberg, R. G. (2016). *Automating condition monitoring of vegetation on railway trackbeds and embankments*. Edinburgh University Press.

Nyberg, R. G., Gupta, N., Yella, S., & Dougherty, M. (2013). Detecting plants on railway embankments. *Journal of Software Engineering and Applications*, *6*(3B), 8–12.

Oude Elberink, S., Khoshelham, K., Arastounia, M., & Díaz Benito, D. (2013). Rail Track

Detection and Modelling in Mobile Laser Scanner Data. *ISPRS Annals of the Photogrammetry, Remote Sensing and Spatial Information Sciences*, *2*(5W2), 223–228. https://doi.org/10.5194/isprsannals-II-5-W2-223-2013

Parente, J., Pereira, M. G., Amraoui, M., & Tedim, F. (2018). Negligent and intentional fires in Portugal: Spatial distribution characterization. *Science of the Total Environment*, *624*, 424–437.

Pastucha, E. (2016). Catenary System Detection, Localization and Classification Using Mobile Scanning Data. *Remote Sensing*, *8*(10), 801. https://doi.org/10.3390/rs8100801

Pimont, F., Dupuy, J.-L., Rigolot, E., Prat, V., & Piboule, A. (2015). Estimating leaf bulk density distribution in a tree canopy using terrestrial LiDAR and a straightforward calibration procedure. *Remote Sensing*, *7*(6), 7995–8018.

Riveiro, B., González-Jorge, H., Martínez-Sánchez, J., Díaz-Vilariño, L., & Arias, P. (2015). Automatic detection of zebra crossings from mobile LiDAR data. *Optics and Laser Technology*. https://doi.org/10.1016/j.optlastec.2015.01.011

Riveiro, Belén, Conde, B., & Arias, P. (2015). Laser Scanning for the Evaluation of Historic Structures. In *Handbook of Research on Seismic Assessment and Rehabilitation of Historic Structures: Vol. i* (pp. 213–256). https://doi.org/10.4018/978-1-4666-8286-3

Riveiro, Belén, Diaz-Vilariño, L., Conde, B., Soilán, M., & Arias, P. (2016). Automatic Segmentation and Shape-Based Classification of Retro-Reflective Traffic Signs from Mobile LiDAR Data. *IEEE Journal of Selected Topics in Applied Earth Observations and Remote Sensing*, *9*(1), 295–303. https://doi.org/10.1109/JSTARS.2015.2461680

Rizaldy, A., Persello, C., Gevaert, C. M., & Oude Elberink, S. J. (2018). Fully Convolutional Networks for Ground Classification from LIDAR Point Clouds. *ISPRS Annals of Photogrammetry, Remote Sensing and Spatial Information Sciences*, *IV–2*, 231–238. https://doi.org/10.5194/isprs-annals-IV-2-231-2018

Rodríguez-Cuenca, B., García-Cortés, S., Ordóñez, C., & Alonso, M. (2016). Morphological Operations to Extract Urban Curbs in 3D MLS Point Clouds. *ISPRS International Journal of Geo-Information*. https://doi.org/10.3390/ijgi5060093

Sadeghi, J., Motieyan Najar, M. E., Zakeri, J. A., & Kuttelwascher, C. (2019). Development of railway ballast geometry index using automated measurement system. *Measurement*, *138*, 132–142. https://doi.org/10.1016/j.measurement.2019.01.092

Sánchez-Rodríguez, A., Riveiro, B., Soilán, M., & González-deSantos, L. M. (2018). Automated detection and decomposition of railway tunnels from Mobile Laser Scanning Datasets. *Automation in Construction*, *96*(April), 171–179. https://doi.org/10.1016/j.autcon.2018.09.014

Sánchez-Rodríguez, Ana, Riveiro, B., Soilán, M., & González-deSantos, L. M. (2018). Automated detection and decomposition of railway tunnels from Mobile Laser Scanning Datasets. *Automation in Construction*, *96*(April), 171–179. https://doi.org/10.1016/j.autcon.2018.09.014

Sánchez-Rodríguez, Ana, Soilán, M., Cabaleiro, M., & Arias, P. (2019). Automated inspection

of Railway Tunnels' power line using LiDAR point clouds. *Remote Sensing*, *11*(21). https://doi.org/10.3390/rs11212567

Schmuck, G., San-Miguel-Ayanz, J., Durrant, T., Boca, R., Libertà, G., Petroliagkis, T., & Schulte, E. (2015). *Forest fires in Europe, Middle East and North Africa 2014. Scientific and Technical Research series-JRC Technical Reports*. Publications Office of the European Union.

Serra, L., Saez, M., Juan, P., Varga, D., & Mateu, J. (2014). A spatio-temporal Poisson hurdle point process to model wildfires. *Stochastic Environmental Research and Risk Assessment*, *28*(7), 1671–1684.

Sherstjuk, V., Zharikova, M., & Sokol, I. (2018). Forest fire-fighting monitoring system based on uav team and remote sensing. *2018 IEEE 38th International Conference on Electronics and Nanotechnology (ELNANO)*, 663–668.

Soilán, M., Nóvoa, A., Sánchez-Rodríguez, A., Riveiro, B., & Arias, P. (2020). Semantic Segmentation of Point Clouds with Pointnet and Kpconv Architectures Applied to Railway Tunnels. *ISPRS Annals of the Photogrammetry, Remote Sensing and Spatial Information Sciences*, *5*(2), 281–288. https://doi.org/10.5194/isprs-annals-V-2-2020-281-2020

Soilán, M., Riveiro, B., Sánchez-Rodríguez, A., & Arias, P. (2018). Safety assessment on pedestrian crossing environments using MLS data. *Accident Analysis and Prevention*, *111*. https://doi.org/10.1016/j.aap.2017.12.009

Soilán, Mario, Justo, A., Sánchez-Rodríguez, A., & Riveiro, B. (2020). 3D point cloud to BIM: Semi-automated framework to define IFC alignment entities from MLS-acquired LiDAR data of highway roads. *Remote Sensing*, *12*(14), 1–22. https://doi.org/10.3390/rs12142301

Soilán, Mario, Riveiro, B., Martínez-Sánchez, J., & Arias, P. (2016). Traffic sign detection in MLS acquired point clouds for geometric and image-based semantic inventory. *ISPRS Journal of Photogrammetry and Remote Sensing*, *114*, 92–101. https://doi.org/10.1016/j.isprsjprs.2016.01.019

Soilán, Mario, Riveiro, B., Martínez-Sánchez, J., & Arias, P. (2017). Segmentation and classification of road markings using MLS data. *ISPRS Journal of Photogrammetry and Remote Sensing*, *123*, 94–103. https://doi.org/10.1016/j.isprsjprs.2016.11.011

Soni, A., Robson, S., & Gleeson, B. (2014). Extracting Rail Track Geometry from Static Terrestrial Laser Scans for Monitoring Purposes. *ISPRS - International Archives of the Photogrammetry, Remote Sensing and Spatial Information Sciences*, *XL–5*(5), 553–557. https://doi.org/10.5194/isprsarchives-XL-5-553-2014

Sousa, J. J., & Bastos, L. (2013). Multi-temporal SAR interferometry reveals acceleration of bridge sinking before collapse. *Natural Hazards and Earth System Sciences*, *13*, 659–667. https://doi.org/10.5194/nhess-13-659-2013

Sterckx, S., Brown, I., Kääb, A., Krol, M., Morrow, R., Veefkind, P., Boersma, K. F., De Mazière, M., Fox, N., & Thorne, P. (2020). Towards a European Cal/Val service for earth observation. In *International Journal of Remote Sensing* (Vol. 41, Issue 12, pp. 4496–

4511). Taylor and Francis Ltd. https://doi.org/10.1080/01431161.2020.1718240

Strozzi, T., Wegmuller, U., Bitelli, G., & Spreckels. (2001). Land Subsidence Monitoring with Differential SAR Interferometry. *Undefined*.

Su, Y., Guo, Q., Fry, D. L., Collins, B. M., Kelly, M., Flanagan, J. P., & Battles, J. J. (2016). A vegetation mapping strategy for conifer forests by combining airborne LiDAR data and aerial imagery. *Canadian Journal of Remote Sensing*, *42*(1), 1–15.

Suresh, D., & Yarrakula, K. (2018). Subsidence monitoring techniques in coal mining: Indian scenario. *Indian Journal of Geo-Marine Sciences*.

Taheri Andani, M., Mohammed, A., Jain, A., & Ahmadian, M. (2018). Application of LIDAR technology for rail surface monitoring and quality indexing. *Proceedings of the Institution of Mechanical Engineers, Part F: Journal of Rail and Rapid Transit*, *232*(5), 1398–1406. https://doi.org/10.1177/0954409717727200

Teledyne Optech ©. (2019). *Teledyne Optech*. http://www.teledyneoptech.com/en/home/

Tonini, M., Pereira, M. G., Parente, J., & Orozco, C. V. (2017). Evolution of forest fires in Portugal: from spatio-temporal point events to smoothed density maps. *Natural Hazards*, *85*(3), 1489–1510.

Vidal, A., Pinglo, F., Durand, H., Devaux-Ros, C., & Maillet, A. (1994). Evaluation of a temporal fire risk index in Mediterranean forests from NOAA thermal IR. *Remote Sensing of Environment*, *49*(3), 296–303.

Viegas, D. X. (2018). Wildfires in Portugal. *Fire Research*.

Vilar, L., Camia, A., San-Miguel-Ayanz, J., & Martín, M. P. (2016). Modeling temporal changes in human-caused wildfires in Mediterranean Europe based on land use-land cover interfaces. *Forest Ecology and Management*, *378*, 68–78.

Vilar, L., Woolford, D. G., Martell, D. L., & Martín, M. P. (2010). A model for predicting human-caused wildfire occurrence in the region of Madrid, Spain. *International Journal of Wildland Fire*, *19*(3), 325–337.

Wang, H., Luo, H., Wen, C., Cheng, J., Li, P., Chen, Y., Cheng Wang, & Li, J. (2015). Road Boundaries Detection Based on Local Normal Saliency From Mobile Laser Scanning Data. *IEEE Geoscience and Remote Sensing Letters*, *12*(10), 2085–2089. https://doi.org/10.1109/LGRS.2015.2449074

Wang, Yanjun, Chen, Q., Liu, L., & Li, K. (2018). A Hierarchical unsupervised method for power line classification from airborne LiDAR data. *International Journal of Digital Earth*, 1–17. https://doi.org/10.1080/17538947.2018.1503740

Wang, Yunsheng, Hyyppä, J., Liang, X., Kaartinen, H., Yu, X., Lindberg, E., Holmgren, J., Qin, Y., Mallet, C., & Ferraz, A. (2016). International benchmarking of the individual tree detection methods for modeling 3-D canopy structure for silviculture and forest ecology using airborne laser scanning. *IEEE Transactions on Geoscience and Remote Sensing*, *54*(9), 5011–5027.

Wang, Z., & Perissin, D. (2012). Cosmo SkyMed AO projects - 3D reconstruction and stability

monitoring of the Three Gorges Dam. *International Geoscience and Remote Sensing Symposium (IGARSS)*, 3831–3834. https://doi.org/10.1109/IGARSS.2012.6350577

Xiao-rui, T., Mcrae, D. J., Li-fu, S., Ming-yu, W., & Hong, L. (2005). Satellite remote-sensing technologies used in forest fire management. *Journal of Forestry Research*, *16*(1), 73–78.

Xie, X., & Lu, X. (2017). Development of a 3D modeling algorithm for tunnel deformation monitoring based on terrestrial laser scanning. *Underground Space (China)*, *2*(1), 16–29. https://doi.org/10.1016/j.undsp.2017.02.001

Xu, S., Xu, S., Ye, N., & Zhu, F. (2018). Automatic extraction of street trees' nonphotosynthetic components from MLS data. *International Journal of Applied Earth Observation and Geoinformation*. https://doi.org/10.1016/j.jag.2018.02.016

Yan, L., Li, Z., Liu, H., Tan, J., Zhao, S., & Chen, C. (2017). Detection and classification of pole-like road objects from mobile LiDAR data in motorway environment. *Optics and Laser Technology*. https://doi.org/10.1016/j.optlastec.2017.06.015

Yang, B., & Fang, L. (2014). Automated Extraction of 3-D Railway Tracks from Mobile Laser Scanning Point Clouds. *IEEE Journal of Selected Topics in Applied Earth Observations and Remote Sensing*, *7*(12), 4750–4761. https://doi.org/10.1109/JSTARS.2014.2312378

Yella, S., & Nyberg, R. G. (2016). Assessing the quality and reliability of visual estimates in determining plant cover on railway embankments. *International Conference on Web Information Systems Engineering*, 404–410.

Yella, S., Nyberg, R. G., Payvar, B., Dougherty, M., & Gupta, N. K. (2013). Machine vision approach for automating vegetation detection on railway tracks. *Journal of Intelligent Systems*, *22*(2), 179–196.

Yu, Y., Li, J., Guan, H., & Wang, C. (2014). 3D crack skeleton extraction from mobile LiDAR point clouds. *International Geoscience and Remote Sensing Symposium (IGARSS)*, 914–917. https://doi.org/10.1109/IGARSS.2014.6946574

Yu, Yongtao, Guan, H., & Ji, Z. (2015). Automated Detection of Urban Road Manhole Covers Using Mobile Laser Scanning Data. *IEEE Transactions on Intelligent Transportation Systems*. https://doi.org/10.1109/TITS.2015.2413812

Yuan, C., Liu, Z., & Zhang, Y. (2017). Fire detection using infrared images for UAV-based forest fire surveillance. *2017 International Conference on Unmanned Aircraft Systems (ICUAS)*, 567–572.

Zai, D., Li, J., Guo, Y., Cheng, M., Lin, Y., Luo, H., & Wang, C. (2018). 3-D Road Boundary Extraction from Mobile Laser Scanning Data via Supervoxels and Graph Cuts. *IEEE Transactions on Intelligent Transportation Systems*. https://doi.org/10.1109/TITS.2017.2701403

Zarembski, A. M., Grissom, G. T., & Euston, T. L. (2014). On the Use of Ballast Inspection Technology For the Management of Track Substructure. *Springer*, *1*(1), 83–109. https://doi.org/10.1007/s40515-014-0004-5

Zhang, I., Yang, F., Zhang, Y., & Zhu, Y. (2016). *Road crack detection using deep Convolutional*

Neural Network.

Zhang, S., Wang, C., Yang, Z., Chen, Y., & Li, J. (2016). Automatic railway power line extraction using mobile laser scanning data. *International Archives of the Photogrammetry, Remote Sensing and Spatial Information Sciences - ISPRS Archives*, *41*(July), 615–619. https://doi.org/10.5194/isprsarchives-XLI-B5-615-2016